Quantum-limited cooling and detection of radio-frequency oscillations by laser-cooled ions

D. J. Heinzen and D. J. Wineland

Time and Frequency Division, National Institute of Standards and Technology, Boulder, Colorado 80303

A single trapped ion, laser cooled into its quantum ground state of motion, may be used as a very-low-temperature detector of radio-frequency signals applied to the trap end caps. If the signal source is a resonant oscillator of sufficiently high Q, the source may also be placed in its quantum ground state by coupling to the ion. Parametric couplings may be used to cool and detect source modes other than the mode directly coupled to the ion. A theoretical analysis of these cooling and detection processes is presented, and as an example, their application to single trapped electron and proton spectroscopy is examined. Squeezing and low noise detection of one quadrature component of the source oscillation are also discussed. The techniques discussed here may lead to radio-frequency measurements of improved accuracy and sensitivity. Cooling and detection of vibrations of macroscopic oscillators also appear possible.

I. INTRODUCTION

Frequently, measurements depend on the detection of weak signals at radio frequencies. An example to be discussed in this paper is the detection of rf currents in pick-up electrodes induced by charged-particle motion. Weak signals must first be amplified to detectable levels. This amplification may be linear, in which case the fundamental limit to signal detection is set by zero-point fluctuations.[1-5] Alternatively, signals may be amplified by "quantum multiplication," in which an absorbed quantum from the signal-carrying field generates a detectable number of secondary quanta, such as occurs in a photomultiplier tube. In measurements using quantum multiplication,[5-7] there is no fundamental lower limit on noise power. However, the signal acquires shot noise since the absorbed energy is quantized; moreover, phase information is lost.

At radio frequencies, sensitivity at the quantum level cannot be achieved with present techniques. That is, linear rf amplifiers add noise far in excess of the quantum-mechanical minimum;[1-5] also, "quantum multipliers" capable of detecting single rf quanta cannot be constructed with conventional techniques. Essentially, this is due to the smallness of $\hbar\omega/k_B$ (48 μK at $\omega/2\pi=1$ MHz), and to coupling of dissipative elements in the amplifier to thermal reservoirs of temperature $T \gg \hbar\omega/k_B$, which introduces excess thermal noise. Here, $2\pi\hbar$ is Planck's constant, ω is the signal-carrier frequency, and k_B is Boltzmann's constant. The best results have been obtained with a superconducting quantum interference device[8,9] (SQUID) and field-effect-transistor[10,11] (FET) amplifiers, both of which exhibit effective noise temperatures[1-5] $T_{\text{eff}} > 0.1$ K $\gg \hbar\omega/k_B$, that preclude quantum-limited sensitivity.

In order to improve the performance of rf amplifiers, circuit elements with much lower dissipation and noise temperature are required. Such low temperature and dissipation may be achieved in the motion of laser-cooled

trapped ions. Recently, a single Hg$^+$ ion harmonically bound in an rf Paul trap[12,13] has been laser cooled to an extent where it spends most of its time in its zero-point (ground) state of motion.[14] (Although this cooling was demonstrated only for two degrees of freedom of the ion's motion, it can straightforwardly be extended to all three degrees of freedom.) As a by-product of this experiment, single rf quanta absorbed by the ion could be detected with high efficiency. In this paper, we further examine how such a laser-cooled ion can function as a sensitive detector of rf signals applied to the trap electrodes. We examine detection based on both linear amplification and quantum multiplication. For ions which are cooled to temperatures less than $\hbar\omega/k_B$, sensitivity at the quantum level may be achieved.

For such a detector to be useful, the signal source must also have a low noise temperature. Most rf sources do not satisfy this condition, but a source consisting of a resonant oscillator mode of very high Q can be cooled to a very low temperature by coupling to the ion. Examples of such resonant source modes might include modes of a bulk wave resonator such as a piezoelectric crystal, electromagnetic cavity or tuned circuit modes, or an ion confined in another trap. We also show that parametric couplings may be used to cool and detect source modes other than the mode directly coupled to the ion. This may be useful if the desired source mode is not easily coupled out electrically or has a much higher or lower frequency than is convenient to match to the ion's frequency.

Since most rf signals are contaminated by noise far in excess of the quantum-mechanical minimum, we envision the primary applications of these ideas to be the cooling and detection of small excitations of such high-Q oscillators. There are at least two situations in which this is useful. First, the oscillator may be driven by a classical field that is strong (containing many quanta per mode) but couples very weakly to the oscillator. Such couplings might include gravity waves,[15-17] or other weak forces.[16,18] Second, it may be that a precise measurement

of the source oscillator's frequency is desired, and that large amplitudes are undesirable because of anharmonic frequency shifts.

When the source mode is the harmonic oscillation of an ion or ions in a separate trap, this technique of "coupled traps" can provide another means to extend laser cooling to ions which cannot be directly laser cooled. Although sympathetic laser cooling[19] has been successfully applied to ions of the same charge in a Penning trap[19,20] and to small numbers of ions in a Paul trap,[21,22] the coupled trap configuration has the potential advantage that the coupling between different ion species can be easily turned on and off (by changing the resonant mode frequencies) and therefore perturbations between ion species can be avoided.

An interesting application of these ideas may be the cooling and detection of excitations of a single electron or proton (or their antiparticles) confined in an ion trap. We show that these particles can be placed in their quantum-mechanical ground state, and single-quantum excitations to any of the particle's degrees of freedom detected. In addition to the aesthetic appeal of finding such a particle in its ground state, this dramatically reduces perturbations to the particle's frequencies of motion.[23-27] This has important implications for the measurement of the electron g factor,[23,27] electron-positron g-factor ratio[27] and mass ratio,[28] proton-antiproton mass ratio,[29] and mass ratios of other ions.[25,26] In addition, a high-precision determination of the proton g factor (and proton-antiproton g-factor ratio) should be possible with use of this technique; this measurement is very difficult with already proven techniques.

It should also be possible to parametrically drive the ion's motion, resulting in noise-free linear amplification[4] of one of its quadrature amplitudes. Thus, if a signal is present in this quadrature, it can be detected with no added noise. In addition, it should be possible to prepare the laser-cooled ion in a squeezed state[4,30-32] by a nonadiabatic change in the ion trap potential or by a parametric drive. A source consisting of a high-Q oscillator mode may then also be prepared in a squeezed state by coupling to the ion. Thus one of the source mode's quadrature amplitudes may be detected with extremely low noise, limited only by the initial degree of squeezing of the ion.

Because this system is conceptually simple, it could serve as a useful paradigm for quantum measurements. Certain concepts, such as squeezing, can be readily visualized. As a practical matter, we think that these ideas will enable rf measurements to be made with improved accuracy and sensitivity.

This paper is organized as follows. In Sec. II, we begin by discussing signal detection by a single ion, in the simplified case in which the ion trap is driven by a voltage source with added thermal noise. We discuss the detection of a single rf quantum by laser sideband cooling and detection of the ion's motion, and derive expressions for the number of signal-induced and thermally induced quanta. In Sec. III, we extend these results to the case in which the signal source is a high-Q oscillator, showing that cooling and detection at nearly the quantum limit may be achieved by coupling to the ion. Cooling and

detection of source modes other than the one directly coupled to the ion via parametric couplings is discussed in Sec. IV. The technique of "coupled-trap spectroscopy," in which the laser-cooled ion is used to cool and detect excitations of a charged particle in a second trap, is introduced in Sec. V. Linear amplification and squeezing of the ion or source oscillator's motion is discussed in Sec. VI. We conclude in Sec. VII.

In Appendices A–C, we further examine the experimental possibilities. A technique for single-quantum detection using Raman transitions is discussed in Appendix A. This technique allows the laser sideband cooling and detection method to be extended to low-mass ions such as $^9Be^+$. This increases the coupling between the source oscillator and the ion, since low-mass ions couple more strongly than high-mass ions. In Appendix B, we analyze an experiment to cool and detect excitations of an electron in a Penning trap with the coupled-trap method. Finally, in Appendix C we examine continuous cooling and the possibility of cooling a mode of a quartz-crystal oscillator.

II. SENSITIVE SIGNAL DETECTION BY A SINGLE ION

We first consider the simplified case in which the ion is driven by a source with purely resistive impedance, as illustrated in Fig. 1. A single ion of charge q_i and mass m_i is confined in a rf trap or Penning trap[12,13,23,27] of endcap separation d_i. For brevity, we consider the detection of a signal by its influence on the ion's motion along the trap symmetry (z) axis. Similar considerations would apply for detection with motion in the x-y plane using a split-ring electrode. The trapping potential along the z axis is assumed to be harmonic and results in an ion axial oscillation frequency ω_i. We model the source as a voltage source u_s, with dissipation in the source represented by a series resistance R_s at temperature T_s. Associated with the source resistance is a noise voltage source u_{ns}. We also assume that the amplitude and phase of the source u_s is classically well defined, but that the source excites the ion only weakly. This will be a valid assumption if u_s is applied for a very short time or is derived
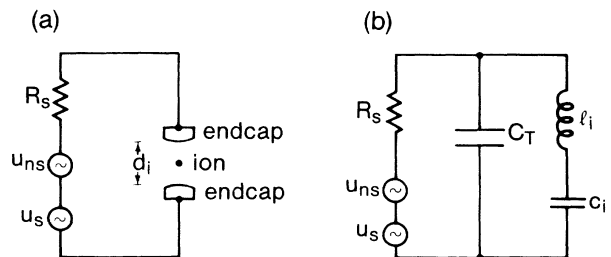

FIG. 1. (a) Single trapped ion driven by a signal source attached to the trap end caps. For simplicity the ring electrode of the ion trap is not shown. (b) Electrical equivalent circuit of the arrangement in (a), where the trapped ion is represented as a series $l_i c_i$ circuit in parallel with the end cap–to–end cap capacitance C_T (Ref. 34).

from a classically strong source which couples very weakly to the ion (due to shielding, for example).

The ion's charge is coupled to the electrical circuit of Fig. 1(a) via the image charges it generates in the end caps. This induced charge is given by[33,34]

$$q_i^{\text{ind}} = \frac{\alpha_i q_i z_i}{d_i} , \tag{1}$$

where z_i is the axial displacement of the ion from its equilibrium position, α_i is a geometrical factor of order unity, and we have assumed the rf wavelength is much larger than the trap dimension. (A voltage V applied across the trap end caps generates an electric field $\alpha_i V/d_i$ at the ion. For traps with hyperbolic-shaped electrodes $\alpha_i \simeq 0.8$.[35]) Because the ion is harmonically bound, it can be shown that the ion and its image current are electrically equivalent to a series $l_i c_i$ circuit which shunts the end caps,[34] with

$$l_i = m_i (d_i/\alpha_i q_i)^2 , \tag{2a}$$

$$c_i = (\omega_i^2 l_i)^{-1} . \tag{2b}$$

Additional forces on the ion from the induced charge q_i^{ind} are assumed to be negligible.[34] The circuit of Fig. 1(a) is therefore electrically equivalent to that shown in Fig. 1(b), where C_T is the capacitance between the trap end caps. The effect of the trap capacitance can be neglected if $R_s \ll (\omega_i C_T)^{-1}$; we assume that this is the case in the remainder of this section.

Neglecting the trap capacitance C_T, the circuit of Fig. 1(b) is a driven simple harmonic oscillator, with the resistance R_s and noise source u_{ns} representing the coupling of the circuit to some thermal reservoir. The behavior of such a damped oscillator is described quantum mechanically by[36]

$$\frac{d\hat{a}_i}{dt} = -\left[i\omega_i + \frac{\gamma}{2}\right]\hat{a}_i + \hat{f}_n(t) + f_s(t) , \tag{3a}$$

$$\frac{d\hat{a}_i^{\dagger}}{dt} = \left[i\omega_i - \frac{\gamma}{2}\right]\hat{a}_i^{\dagger} + \hat{f}_n^{\dagger}(t) + f_s^*(t) , \tag{3b}$$

where $\hat{a}_i^{\dagger}$ and $\hat{a}_i$ are the creation and annihilation operators for a quantum of oscillation; they are related to the charge $\hat{q}_i^{\text{ind}}$ on the capacitor c_i by

$$\hat{q}_i^{\text{ind}} = \left[\frac{\hbar}{2\omega_i l_i}\right]^{1/2} (\hat{a}_i^{\dagger} + \hat{a}_i) . \tag{4}$$

Here $\gamma = R_s/l_i$ is the damping rate for the oscillator, and $\hat{f}_n(t)$ and $\hat{f}_n^{\dagger}(t)$ are noise operators, which satisfy[36]

$$\langle \hat{f}_n(t) \rangle = \langle \hat{f}_n^{\dagger}(t) \rangle = 0 , \tag{5}$$

$$\langle \hat{f}_n^{\dagger}(t_1)\hat{f}_n(t_2) \rangle = \gamma \bar{n}\delta(t_1 - t_2) , \tag{6a}$$

$$\langle \hat{f}_n(t_1)\hat{f}_n^{\dagger}(t_2) \rangle = \gamma(\bar{n} + 1)\delta(t_1 - t_2) , \tag{6b}$$

where the brackets denote an average over the thermal reservoir states, and

$$\bar{n} = \frac{1}{e^{\hbar\omega_i/k_B T_s} - 1} \tag{7}$$

is the number of quanta in the circuit in thermal equilibrium. The effect of the noise voltage source u_{ns} is included via the terms $f_n(t)$ and $f_n^{\dagger}(t)$. The drive is included via the term $f_s(t)$, which is assumed to be classical. For the case of a resonant drive of the form $u_s = \text{Re}(u_{s0}e^{-i\omega_i t})$,

$$f_s = iu_{s0}e^{-i\omega_i t}(8\hbar\omega_i l_i)^{-1/2} .$$

From Eq. (3a), we find that

$$\hat{a}_i(t) = \hat{a}_i(0)e^{-(i\omega_i + \gamma/2)t}$$
$$+ \int_0^t [\hat{f}_n(t_1) + f_s(t_1)]e^{-(i\omega_i + \gamma/2)(t - t_1)}dt_1 , \tag{8}$$

and the corresponding conjugate equation for $\hat{a}^{\dagger}$.

For simplicity, we assume that u_s is a resonant pulse of duration t_m. We find that

$$\hat{a}_i(t_m) = \hat{a}_i(0)e^{-(i\omega_i + \gamma/2)t_m}$$
$$+ \int_0^{t_m} \hat{f}_n(t_1)e^{-(i\omega_i + \gamma/2)(t_m - t_1)}dt_1$$
$$+ \frac{iu_{s0}e^{-i\omega_i t_m}(1 - e^{-\gamma t_m/2})}{(2\hbar\omega_i \gamma^2 l_i)^{1/2}} . \tag{9}$$

From Eq. (9) we see that the oscillator's amplitude contains a term proportional to the drive amplitude u_{s0}. This amplitude contribution may be detected directly by a linear parametric amplification technique discussed in Sec. VI.

Alternatively, we may detect the absorbed vibrational quanta. We find that the mean number of quanta $\langle \hat{n}_i \rangle = \langle \hat{a}_i^{\dagger}\hat{a}_i \rangle$ in the circuit at time t_m is given by

$$\langle \hat{n}_i(t_m) \rangle = \langle \hat{n}_i(0) \rangle e^{-\gamma t_m} + \bar{n}(1 - e^{-\gamma t_m})$$
$$+ \frac{|u_{s0}|^2}{2\hbar\omega_i \gamma^2 l_i}(1 - e^{-\gamma t_m/2})^2 , \tag{10a}$$

where we have neglected possible coherence of the initial state; that is, we assume that $\langle \hat{a}(0) \rangle = \langle \hat{a}^{\dagger}(0) \rangle = 0$. The three terms on the right-hand side of Eq. (10a) describe the decay of initial quanta stored in the circuit, the buildup of "blackbody" quanta in the circuit, and the buildup of "signal" quanta. For $t_m \ll \gamma^{-1}$,

$$\langle \hat{n}_i(t_m) \rangle \simeq \langle \hat{n}_i(0) \rangle + \gamma \bar{n}t_m + \frac{|u_{s0}|^2 t_m^2}{8\hbar\omega_i l_i} . \tag{10b}$$

Single-quantum excitations in the circuit representing the ion's motion may be detected via the method outlined in Refs. 14 and 37 and as illustrated in Fig. 2. To summarize the method, we first assume that the ion's internal structure has a ground state $|g\rangle$ which is weakly coupled to an excited state $|w\rangle$, which slowly decays to $|g\rangle$ at a rate γ_w. Also, $|g\rangle$ is strongly coupled to an excited state $|s\rangle$, which rapidly decays to $|g\rangle$ at a rate $\gamma_s \gg \gamma_w$. We assume that $\gamma_w \ll \omega_i$, so that the combined internal-translational quantum states of the ion for levels $|g\rangle$ and $|w\rangle$ consist of well-resolved ladders of states $|g,n_i\rangle$ and $|w,n_i\rangle$, with $n_i = 0,1,2,\ldots$. We also assume that $R \ll \hbar\omega_i$, where $R = (\hbar k)^2/2m$ is the recoil energy, with
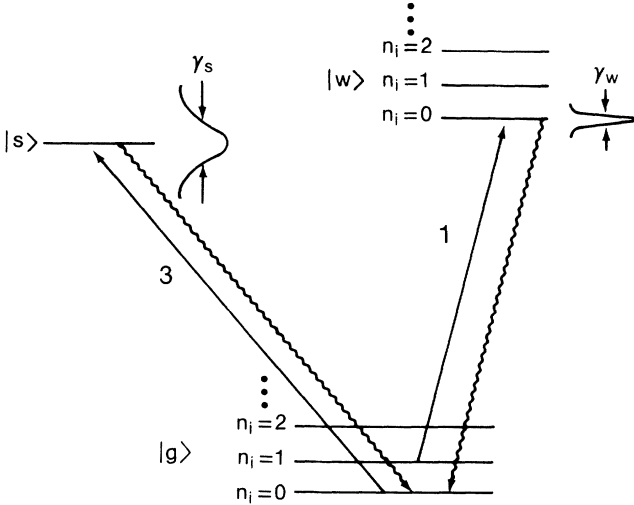
FIG. 2. Sideband cooling and detection of a single trapped ion. The sideband cooling laser (1) is tuned to the first lower sideband of the $|g\rangle \rightarrow |w\rangle$ transition and primarily induces transitions of the type $|g,n_i\rangle \rightarrow |w,n_i-1\rangle$. The detection laser (3) primarily induces transitions of the form $|g,n_i\rangle \rightarrow |s,n_i\rangle$. Observation of the absence of fluorescence from this transition indicates that the ion is in the $|w\rangle$ state. (Dehmelt's electron shelving scheme, Ref. 7.)

k the wave number of the weak transition. The ion is cooled by tuning a laser to the first lower sideband at $\omega_{wg} - \omega_i$, where ω_{wg} is the $|g\rangle \rightarrow |w\rangle$ transition frequency of an atom held at rest. This induces $\Delta n_i = -1$ transitions in the ion, with spontaneous decays back to level $|g\rangle$ occurring predominantly with $\Delta n_i = 0$. The ion is therefore optically pumped down the ladder of states until it reaches $n_i = 0$ with high probability, at which point it interacts very weakly with the laser.[37-38] A more detailed analysis of the sideband cooling process leads to a limit on $\langle n_i(0)\rangle = f\gamma_w^2/\omega_i^2$, where f is a constant of order unity.[37-38]

Single-quantum excitations from $|g,n_i=0\rangle$ to $|g,n_i=1\rangle$ may be detected by first applying a π pulse[40] of radiation to the $|g,n_i=1\rangle$ to $|w,n_i=0\rangle$ transition. If the ion was initially in the $|g,n_i=1\rangle$ state, it is therefore transferred to the excited state $|w\rangle$, where it remains for a time of order γ_w^{-1}. If it was initially in the $|g,n_i=0\rangle$ state, it remains in the state $|g\rangle$.[14,37] Then a strong pulse of radiation is applied on the $|g\rangle \leftrightarrow |s\rangle$ transition of duration t_d such that $\gamma_s^{-1} \ll t_d \ll \gamma_w^{-1}$. During this time, many photons are scattered and detected if the ion was initially in $|g,n_i=0\rangle$. If it was initially in the state $|g,n_i=1\rangle$, it remains in the state $|w\rangle$ during the time t_d and scatters no photons. High sensitivity of detection of the $|w\rangle$ state is achieved because of the absence of many scattered photons during the time t_D. This is an example of the quantum multiplication provided by "electron shelving" of the ion.[7,41-44] This sideband cooling and detection scheme has recently been demonstrated experimentally.[14] (The work of Ref. 14 differs slightly in that the π pulses on the $|g,n_i=1\rangle$ to $|w,n_i=0\rangle$ transition were not used.)

For this single-quantum detection method to be useful,

it is necessary to avoid saturating the detector with thermally induced quanta. Since typically $\bar{n} \gg 1$, this implies that we must have $\gamma t_m < 1/\bar{n} \ll 1$. In this case, the signal-to-background ratio is

$$\left|\frac{S}{B}\right| = \frac{n_s}{\langle \hat{n}_i(0)\rangle + n_{th}} ,$$ (11)

where $n_s = |u_{s0}|^2 t_m^2/8\hbar\omega_i l_i$ and $n_{th} = \gamma \bar{n} t_m$. The noise will be due to fluctuations (shot noise) in the number of either the signal or background quanta. For example, assume that $\langle \hat{n}_i(0)\rangle$, $n_{th} \ll n_s \ll 1$. Then the noise is dominated by the shot noise of the signal. After N measurement cycles, on the average we detect Nn_s excitations to $n_i = 1$, where the rms fluctuations in this number are given by $[Nn_s(1-n_s)]^{1/2} \simeq (Nn_s)^{1/2}$. Therefore the signal-to-noise ratio after N measurements is $(S/N)_N \simeq (Nn_s)^{1/2}$. We note that this shot-noise limitation may be overcome by using the parametric amplification techniques discussed in Sec. VI.

If $n_{th}(t_m) > 1$ or $n_s(t_m) > 1$, it may be desirable to reduce the interaction time to a time t_m', such that $n_{th}(t_m') \ll 1$ and $n_s(t_m') < 1$, although this reduces the ratio n_s/n_{th} by the factor t_m'/t_m. Alternatively, it may be desirable to consider methods to detect final states with $\langle n_i(t_m)\rangle \gg 1$. One method would be to monitor a decrease in fluorescence from the ion due to increased Doppler broadening or to reduced spatial overlap with the exciting laser beam.[24]

Although for simplicity we have considered the ion to be directly driven by a signal source, similar considerations hold when a separate high-Q oscillator is driven by an oscillatory signal and the resulting excitation transferred to the ion for detection, as will be discussed in Sec. III. In this case, the buildup of excitation in the separate oscillator is also described by Eqs. (3)-(10), where γ and $\bar{n}$ now refer to the damping rate and equilibrium number of thermal quanta of the oscillator, and we replace l_i by the oscillator's effective inductance l_s. The oscillating drive need not be electromagnetic; the example of a piezoelectric crystal is discussed in Appendix C. The use of such high-Q oscillators as sensitive detectors of oscillating forces has been discussed in Refs. 15-18.

III. REFRIGERATION AND SENSITIVE DETECTION OF EXCITATION IN A SECOND RESONANT SYSTEM

In this section, we consider a source consisting of a single oscillator mode of sufficiently high Q, such that damping into external reservoirs may be neglected over times of interest. In this case, the source and laser-cooled ion behave simply as a pair of coupled oscillators, and, in the weak damping limit considered here, oscillatory exchange of energy between the two oscillators may be expected. Under these conditions, the ion itself may be used to both cool and detect excitations in the source.

This process may be modeled by the equivalent circuit shown in Fig. 3. As before, l_i and c_i are the effective inductance and capacitance of the trapped ion. The source oscillator may be modeled by a series $l_s c_s$ circuit, with resonant frequency $\omega_s = (l_s c_s)^{-1/2}$. Any parallel source reactance may be included in the capacitance C_T. In gen-
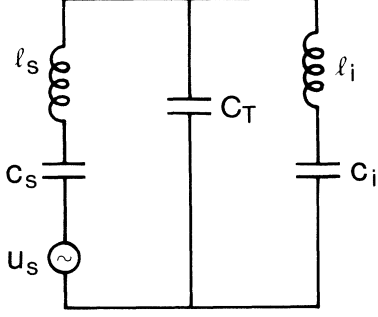
FIG. 3. Equivalent circuit for a single trapped ion coupled to a particular mode of a source oscillator represented by a series $l_s c_s$ circuit.

eral, the source oscillator will in turn be driven by a signal represented here by the voltage source u_s; for the moment, we assume that $u_s = 0$.

The Hamiltonian for the circuit of Fig. 3 may be written as

$$H = \hbar\omega_s'(\hat{a}_s^\dagger \hat{a}_s + \tfrac{1}{2}) + \hbar\omega_i'(\hat{a}_i^\dagger \hat{a}_i + \tfrac{1}{2}) + (m_i m_s)^{1/2} g^2 \hat{x}_s \hat{x}_i \ , \tag{12}$$

where

$$g^2 = (l_s l_i C_T^2)^{-1/2} \ , \tag{13}$$

$c_j' = c_j C_T/(c_j + C_T)$, $\omega_j' = (l_j c_j')^{-1/2}$, with $j = s$ or i, and it is assumed that the total charge in the circuit is zero. As usual, we define operators $\hat{p}_j$ and $\hat{x}_j$ in terms of the raising and lowering operators for oscillator j:

$$\hat{x}_j = \left[\frac{\hbar}{2m_j \omega_j'} \right]^{1/2} (\hat{a}_j^\dagger + \hat{a}_j) \ , \tag{14a}$$

$$\hat{p}_j = i \left[\frac{\hbar m_j \omega_j'}{2} \right]^{1/2} (\hat{a}_j^\dagger - \hat{a}_j) \ . \tag{14b}$$

The "mass" m_j is related to the charge $\hat{q}_j^{\text{ind}}$ on the capacitor c_j by $\hat{q}_j^{\text{ind}} = (m_j/l_j)^{1/2} \hat{x}_j$. (For an ion's axial oscillation, $m_j \equiv m_i$ is the ion mass.) The Heisenberg equations of motion for $\hat{x}_j$ with the Hamiltonian of Eq. (12) are

$$\frac{d^2 \hat{x}_s}{dt^2} + (\omega_s')^2 \hat{x}_s = -g^2 \left[\frac{m_i}{m_s} \right]^{1/2} \hat{x}_i \ , \tag{15a}$$

$$\frac{d^2 \hat{x}_i}{dt^2} + (\omega_i')^2 \hat{x}_i = -g^2 \left[\frac{m_s}{m_i} \right]^{1/2} \hat{x}_s \ . \tag{15b}$$

The general solution to Eqs. (15) is oscillatory, with frequencies $\omega_\pm$ given by

$$\omega_\pm^2 = \tfrac{1}{2}[(\omega_s')^2 + (\omega_i')^2] \pm \tfrac{1}{2}\{[(\omega_s')^2 - (\omega_i')^2]^2 + 4g^4\}^{1/2} \ . \tag{16}$$

We focus here on the case $(|\omega_i' - \omega_s'|\bar{\omega})^{1/2} \ll g \ll \omega_i', \omega_s'$, where $\bar{\omega} = (\omega_+ + \omega_-)/2 \simeq \omega_i' \simeq \omega_s'$. The solutions of Eqs. (15) become

$$\hat{x}_s(t) = \left[\left[\hat{x}_s(0)\cos(\bar{\omega}t) + \frac{\hat{p}_s(0)}{m_s\bar{\omega}}\sin(\bar{\omega}t) \right] \cos(\omega_{\text{ex}}t) \right.$$
$$+ \left[-\hat{x}_i(0)\sin(\bar{\omega}t) + \frac{\hat{p}_i(0)}{m_i\bar{\omega}}\cos(\bar{\omega}t) \right]$$
$$\left. \times \left[\frac{m_i}{m_s} \right]^{1/2} \sin(\omega_{\text{ex}}t) \right. , \tag{17a}$$

$$\hat{x}_i(t) = \left[\left[\hat{x}_i(0)\cos(\bar{\omega}t) + \frac{\hat{p}_i(0)}{m_i\bar{\omega}}\sin(\bar{\omega}t) \right] \cos(\omega_{\text{ex}}t) \right.$$
$$+ \left[-\hat{x}_s(0)\sin(\bar{\omega}t) + \frac{\hat{p}_s(0)}{m_s\bar{\omega}}\cos(\bar{\omega}t) \right]$$
$$\left. \times \left[\frac{m_s}{m_i} \right]^{1/2} \sin(\omega_{\text{ex}}t) \right. , \tag{17b}$$

where

$$\omega_{\text{ex}} = \tfrac{1}{2}(\omega_+ - \omega_-) \simeq \frac{\bar{\omega}(c_i' c_s')^{1/2}}{2C_T} \simeq \frac{1}{2\bar{\omega}(l_i l_s)^{1/2}C_T} \ , \tag{18a}$$

and where we define

$$t_{\text{ex}} = \pi/2\omega_{\text{ex}} = \pi\bar{\omega}(l_i l_s)^{1/2}C_T \ . \tag{18b}$$

Equations (17) describe an oscillatory exchange of excitation between the two oscillators. In particular, for time $t \ll t_{\text{ex}}$ we find that

$$\hat{x}_s(t) \simeq \hat{x}_s(0)\cos(\bar{\omega}t) + \frac{\hat{p}_s(0)}{m_s\bar{\omega}}\sin(\bar{\omega}t) \ , \tag{19a}$$

$$\hat{x}_i(t) \simeq \hat{x}_i(0)\cos(\bar{\omega}t) + \frac{\hat{p}_i(0)}{m_i\bar{\omega}}\sin(\bar{\omega}t) \ . \tag{19b}$$

Whereas, for times $|t - t_{\text{ex}}| \ll t_{\text{ex}}$, we find that

$$\hat{x}_s(t) \simeq \left[\frac{m_i}{m_s} \right]^{1/2} \left[\hat{x}_i(0)\cos\left[\bar{\omega}t + \frac{\pi}{2}\right] \right.$$
$$\left. + \frac{\hat{p}_i(0)}{m_i\bar{\omega}}\sin\left[\bar{\omega}t + \frac{\pi}{2}\right] \right] \ , \tag{20a}$$

$$\hat{x}_i(t) \simeq \left[\frac{m_s}{m_i} \right]^{1/2} \left[\hat{x}_s(0)\cos\left[\bar{\omega}t + \frac{\pi}{2}\right] \right.$$
$$\left. + \frac{\hat{p}_s(0)}{m_s\bar{\omega}}\sin\left[\bar{\omega}t + \frac{\pi}{2}\right] \right] \ . \tag{20b}$$

At time $t = t_{\text{ex}}$, the $\hat{x}_j$ operators have exactly interchanged values, apart from an amplitude factor and phase shift of $\pi/2$. Further, the $\hat{p}_j$ operators have also interchanged values, apart from an amplitude factor and identical phase shift. It then follows that at time $t \simeq t_{\text{ex}}$, the source and ion oscillators have exactly interchanged wave functions, apart from a phase shift of $\pi/2$. (This may be proved explicitly in the Schrödinger picture.)

This oscillatory exchange between the two oscillators suggests the following scheme for cooling the signal

source, as illustrated in Fig. 4(a). The coupling between the two oscillators may be switched on and off by rapidly (compared with t_{ex}) switching the resonant frequencies of the ion oscillator on or off resonance with the source oscillator. Initially both ion and source are assumed to be hot ($(\langle n_s \rangle, \langle n_i \rangle \gg 1)$ [Fig. 4(a) (i)]. First, with the oscillators decoupled, the ion is cooled to the zero-point state using sideband cooling [Fig. 4(a) (ii)]. The cooling laser is then turned off, and the ion and source coupling is switched on for a time t_{ex}, at which time the ion's zero-

point state has been transferred to the source [Fig. 4(a) (iii)]. Finally, at $t = t_{ex}$ the coupling is switched off, and the ion is again cooled to the zero-point state, leaving both ion and source in the ground state [Fig. 4(a) (iv)]. Because the oscillators may be anharmonic, this may take several such cooling cycles depending on the initial values of $\langle n_s \rangle$ and $\langle n_i \rangle$.

The same idea may be used to detect single-quantum excitations to the source oscillator, as illustrated, in Fig. 4(b). The source and ion are initially cooled into the
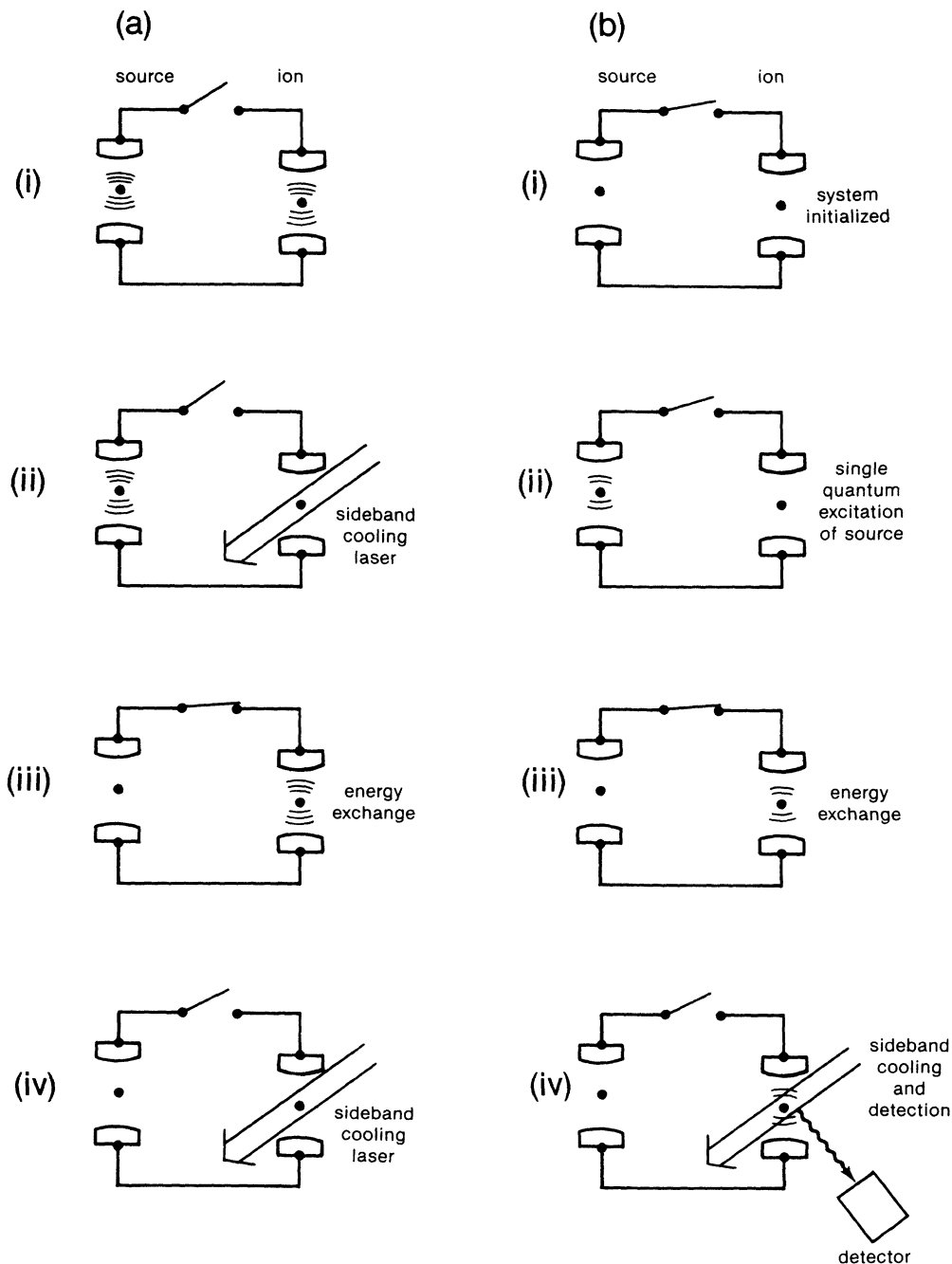

FIG. 4. (a) Cooling of a source to the zero-point state by exchange of energy with an ion which has been laser cooled to the zero-point state. (b) Detecting single-quantum excitations of the source.

zero-point state with the coupling turned off, as in Fig. 4(b) (i). We suppose that the external drive u_s is applied to the source oscillator, which puts at least one quantum of energy into its motion [Fig. 4(b) (ii)]. Then the source and ion are recoupled for a time t_{ex}, resulting in the transfer of the source excitation to the ion [Fig. 4(b) (iii)]. Finally, the excitation of the ion is probed using the side-band method [Fig. 4(b) (iv)].

It should be emphasized that if the signal u_s is continuous and monochromatic, the signal-to-noise ratio is maximized when the source oscillator is driven for times of the order of its relaxation time [see Eqs. (10)]. Then, the source oscillator is contaminated by thermal noise at its equilibrium temperature T_s, and the single-quantum detection technique is not useful. However, this technique should be of advantage whenever the bandwidth of the drive signal is large compared with the source oscillator damping rate. For example, the signal incident on a resonant gravity wave detector may consist of finite duration pulses, rather than a steady drive.[15,16] This technique should also be useful when the signal energy comes from a spin system, which can store only a finite number of quanta (see Sec. V). In each of these cases, the signal-to-noise ratio can be increased by detecting the driven source oscillator's energy against a much lower thermal background.

An additional consideration is that a large source energy may introduce undesirable perturbations to the source. An example, to be discussed further in Sec. V, is the measurement of the cyclotron frequency of a second trapped particle. Most of the important perturbations to the cyclotron frequency, such as anharmonic and relativistic shifts, scale in proportion to the particle energy. Thus, even though a large signal-to-noise ratio is in principle available by applying a large steady drive, the accuracy of the measurement may be degraded by the large energy. The technique described here allows for efficient signal detection at the lowest possible energies, minimizing such perturbations.

The buildup of thermal quanta in an oscillator is described by Eqs. (10). If the present cooling and detection technique is to prove useful, the number of thermally induced quanta $\gamma \bar{n} t_m$ must be less than one, where t_m is the duration of a cooling or measurement cycle. This means that the quality factor $Q = \omega/\gamma$ of the oscillator must satisfy

$$Q > \bar{n}\omega t_m = (kT_s/\hbar)t_m , \qquad (21)$$

where the equality holds for $kT \gg \hbar\omega$. For example, at $T_s = 4.2$ K and $t_m = 0.02$ s, we require $Q > 10^{10}$. Such high Q's can be achieved in the motion of trapped ions.[12-14] Given the progress that has been made with superconducting cavities and crystal oscillators,[16,17] it may be possible to satisfy inequality (21) for these systems as well. Note that if Q is sufficiently large, the large heat capacity of a macroscopic object such as a crystal oscillator is irrelevant, since only vibrations of a single mode are cooled, not the crystal as a whole.

IV. PARAMETRIC COUPLING OF INTERNAL SOURCE MODES

Parametric coupling of two modes can exchange energy between them with no added noise.[1] Thus the cooling and detection techniques described in the previous section may be extended to other source oscillator modes through parametric couplings. To this end we assume that during a time over which the parametric drive is applied, the Hamiltonian of the source may be written as[1]

$$H = (\hat{a}_1^\dagger \hat{a}_1 + \tfrac{1}{2})\hbar\omega_1 + (\hat{a}_2^\dagger \hat{a}_2 + \tfrac{1}{2})\hbar\omega_2$$
$$+ (m_1 m_2)^{1/2} g^2 \cos(\omega_d t)\hat{x}_1 \hat{x}_2 , \qquad (22)$$

where $\hat{x}_j$ and $\hat{p}_j$ are given by Eqs. (14) with $\omega_j' = \omega_j$, and the third term represents the parametric coupling between two of the source modes, modes 1 and 2, with a frequency ω_d and strength g^2. The parametric drive may be assumed to be classical.[1] It is assumed that the couplings between modes 1 or 2 and all other source modes may be neglected. The Heisenberg equations of motion of $\hat{x}_j$ for the Hamiltonian (22) may be written as

$$\frac{d^2\hat{x}_1}{dt^2} + \omega_1^2 \hat{x}_1 = -g_1^2 \left[\frac{m_2}{m_1}\right]^{1/2} \cos(\omega_d t)\hat{x}_2 , \qquad (23a)$$

$$\frac{d^2 x_2}{dt^2} + \omega_2^2 \hat{x}_2 = -g_2^2 \left[\frac{m_1}{m_2}\right]^{1/2} \cos(\omega_d t)\hat{x}_1 , \qquad (23b)$$

where, in the present case, $g_1^2 = g_2^2 = g^2$ (a case where $g_1^2 \neq g_2^2$ is treated below). For maximum parametric coupling of the two modes, we require $\omega_d = \omega_1 - \omega_2$. Defining new slowly varying operators $\tilde{x}_j(t)$ by $\hat{x}_j(t) = \mathrm{Re}[\tilde{x}_j(t)e^{i\omega_j t}]$, substituting for $\hat{x}_j$ and ω_d in Eqs. (23), assuming $g \ll \omega_1, \omega_2$, and keeping only secular terms, we find that

$$\frac{d\tilde{x}_1}{dt} \simeq \frac{ig_1^2}{4\omega_1} \left[\frac{m_2}{m_1}\right]^{1/2} \tilde{x}_2 , \qquad (24a)$$

$$\frac{d\tilde{x}_2}{dt} \simeq \frac{ig_2^2}{4\omega_2} \left[\frac{m_1}{m_2}\right]^{1/2} \tilde{x}_1 . \qquad (24b)$$

Thus noting that $\tilde{x}_j(0) = \hat{x}_j(0) - i\hat{p}_j(0)/m_j\omega_j$, we find that the solutions for $\hat{x}_1$ and $\hat{x}_2$ are

$$\hat{x}_1(t) \simeq \left[\hat{x}_1(0)\cos\omega_1 t + \frac{\hat{p}_1(0)}{m_1\omega_1}\sin\omega_1 t\right]\cos\omega_{ex} t$$
$$+ \left[-\hat{x}_2(0)\sin\omega_1 t + \frac{\hat{p}_2(0)}{m_2\omega_2}\cos\omega_1 t\right]$$
$$\times \left[\frac{m_2\omega_2 g_1^2}{m_1\omega_1 g_2^2}\right]^{1/2} \sin\omega_{ex} t , \qquad (25a)$$

$$\hat{x}_2(t) \simeq \left[\hat{x}_2(0)\cos\omega_2 t + \frac{\hat{p}_2(0)}{m_2\omega_2}\sin\omega_2 t\right]\cos\omega_{ex} t$$
$$+ \left[-\hat{x}_1(0)\sin\omega_2 t + \frac{\hat{p}_1(0)}{m_1\omega_1}\cos\omega_2 t\right]$$
$$\times \left[\frac{m_1\omega_1 g_2^2}{m_2\omega_2 g_1^2}\right]^{1/2} \sin\omega_{ex} t , \qquad (25b)$$

where $\omega_{ex} = g_1 g_2 / 4 (\omega_1 \omega_2)^{1/2}$.

These equations are essentially the same as Eqs. (17), apart from the factor $(m_i \omega_i / \omega_j \omega_j)^{1/2}$ multiplying the $\sin(\omega_{ex} t)$ terms. Thus the same conclusion may be reached regarding the exchange oscillation: Apart from a phase shift of $\pi/2$, oscillators 1 and 2 exactly exchange wave functions when the drive has been applied for a time $t_{ex} = \pi / 2\omega_{ex}$. The factor $(m_i \omega_i / m_j \omega_j)^{1/2}$ normalizes the exchanged wave functions so that the number of quanta are conserved; that is, if $|\psi_1(t=0)\rangle$ has an expansion in terms of the number states of oscillator 1, then $|\psi_2(t=t_{ex})\rangle$ has the same expansion in terms of the number states of oscillator 2, apart from a phase shift.

Equations (25) have important implications for a source coupled to a trapped ion. Suppose that the source is such that only source mode 1 can be efficiently coupled to the ion, but it is desired to measure excitations in source mode 2. Then, according to Eqs. (25), source mode 1 can first be cooled to the $\langle n_1 \rangle = 0$ state, and this state parametrically transferred to source mode 2, so that $\langle n_2 \rangle = 0$. We assume that source mode 1 is then recooled to $\langle n_1 \rangle = 0$. With the parametric drive off, mode 2 may be excited by a signal drive. The excitation in mode 2 may be parametrically transferred to mode 1 and then to the laser-cooled ion for detection. Thus parametric drives may be used to extend the single-quantum detection to source modes other than the one directly coupled to the ion.

V. APPLICATION TO COOLING AND DETECTION OF AN ELECTRON, POSITRON, PROTON, OR ANTIPROTON IN A PENNING TRAP

As an application of the preceding ideas, we consider the measurement of the cyclotron frequency of an electron, a proton or their antiparticles in a Penning trap. The Penning trap consists of a ring electrode and two end-cap electrodes, which to a good approximation produces a potential (in cylindrical coordinates) of the form

$$\phi(\mathbf{r}) = \frac{m\omega_z^2}{2q}(z^2 - \tfrac{1}{2}r^2) , \tag{26}$$

where m, ω_z, and q are the mass, axial frequency, and charge of the trapped particle.[12,13,23,27] Superimposed on the electrostatic potential is a uniform magnetic field $\mathbf{B} = B\hat{z}$, which provides radial confinement of the particle. The Hamiltonian of a single electron in a Penning trap may be written as[23]

$$H_0 = (\hat{n}_z + \tfrac{1}{2})\hbar\omega_z + (\hat{n}_c + \tfrac{1}{2})\hbar\omega_c' - (\hat{n}_m + \tfrac{1}{2})\hbar\omega_m + \tfrac{1}{2}\hbar\omega_s \hat{\sigma}_z , \tag{27}$$

where $\hat{n}_j = \hat{a}_j^\dagger \hat{a}_j$ ($j = z, c,$ or m), and

$$\omega_c' = \frac{\omega_c}{2} + \left[\frac{\omega_c^2}{4} - \frac{\omega_z^2}{2} \right]^{1/2} , \tag{28a}$$

$$\omega_m = \frac{\omega_c}{2} - \left[\frac{\omega_c^2}{4} - \frac{\omega_z^2}{2} \right]^{1/2} . \tag{28b}$$

Here, $\omega_s = (g/2)\omega_c$, with g the electron g factor, $\hat{\sigma}_z$ is the

electron's z component of spin, with eigenvalues ± 1, and $\omega_c = eB/mc$ is the unperturbed cyclotron frequency of the electron.

The electron has four independent degrees of freedom: an axial oscillation at frequency ω_z, a cyclotron motion (perturbed by the trap electric field) at frequency ω_c', a circular magnetron drift about the z axis at frequency ω_m, and the spin. The magnetron oscillator is inverted, corresponding to the instability of the magnetron motion in the trap.

In terms of the $\hat{a}_j$ and $\hat{a}_j^\dagger$, we may also define the operators[45]

$$\hat{z} = \left[\frac{\hbar}{2m\omega_z} \right]^{1/2} (\hat{a}_z^\dagger + \hat{a}_z) , \tag{29a}$$

$$\hat{p}_z = i \left[\frac{\hbar m \omega_z}{2} \right]^{1/2} (\hat{a}_z^\dagger - \hat{a}_z) , \tag{29b}$$

$$\hat{\rho}_c = \left[\frac{\hbar}{m\Omega} \right]^{1/2} (\hat{a}_c^\dagger + \hat{a}_c) , \tag{29c}$$

$$\hat{\pi}_c = i\omega_c' \left[\frac{\hbar m}{\Omega} \right]^{1/2} (\hat{a}_c^\dagger - \hat{a}_c) , \tag{29d}$$

$$\hat{\rho}_m = \left[\frac{\hbar}{m\Omega} \right]^{1/2} (\hat{a}_m^\dagger + \hat{a}_m) , \tag{29e}$$

$$\hat{\pi}_m = -i\omega_m \left[\frac{\hbar m}{\Omega} \right]^{1/2} (\hat{a}_m^\dagger - \hat{a}_m) , \tag{29f}$$

$$\hat{x} = \tfrac{1}{2}(\hat{\rho}_c + \hat{\rho}_m) , \tag{29g}$$

$$\hat{y} = \frac{1}{2m} \left[\frac{\hat{\pi}_c}{\omega_c'} + \frac{\hat{\pi}_m}{\omega_m} \right] , \tag{29h}$$

where $\Omega = (\omega_c' - \omega_m)/2$.

For reasonable experimental parameters, the electron's cyclotron frequency will lie in the GHz range, while the laser-cooled ion's axial frequency will lie in the MHz range. Therefore the desired cyclotron mode cannot be coupled directly to the ion. In order to cool and detect the electron, we connect the end caps of the electron trap to the end caps of the ion trap and adjust the trap voltages, so that the axial frequency of the electron ω_z equals the axial frequency of the ion ω_i. (We might also consider coupling the electronic axial resonance to the ion's cyclotron resonance by splitting the ion trap's ring electrode.) In this case, the two axial oscillators are equivalent to the circuit of Fig. 3, where $u_s = 0$, C_T is the combined capacitance of the two traps in parallel, l_i and c_i are given in Eqs. (2), $l_s = m(d_e/\alpha_e e)^2$, $c_s = (\omega_z^2 l_s)^{-1}$, d_e is the electron end cap separation, and α_e a constant of order unity.[35] Therefore the discussion of Sec. III applies; and it follows that if the ion is prepared in an initial $\langle \hat{n}_i \rangle = 0$ state, this state is transferred to the electron's axial oscillation by allowing them to couple freely for a time $t_{ex} = \pi\omega_z (l_s l_i)^{1/2} C_T$. The axial oscillators can be decoupled by rapidly (but adiabatically) changing the ion trap potential, so that $|\omega_i - \omega_z| \gg [\omega_z (l_s l_i)^{1/2} C_T]^{-1}$.

The electron's other two degrees of freedom, the cyclo-

tron and magnetron motion, may each be coupled parametrically to the axial motion in the manner discussed in Sec. IV. This problem has also been considered and demonstrated in the classical regime by Cornell et al.[46] We consider an applied field of the form

$$\phi(\mathbf{r}) = \frac{E_0}{d} xz \cos\omega_d t \ , \tag{30}$$

with $\mathbf{E} = -\nabla\phi$. Again, the drive may be assumed to be classical.[1] The applied potential gives rise to an additional contribution to the Hamiltonian,

$$H_{\text{int}} = \frac{eE_0}{d}\hat{x}\hat{z}\cos\omega_d t \ . \tag{31}$$

The Heisenberg equations of motion of $\hat{\rho}_c$, $\hat{\rho}_m$, and $\hat{z}$ for the total Hamiltonian $H = H_0 + H_{\text{int}}$ are

$$\frac{d^2\hat{\rho}_c}{dt^2} + (\omega_c')^2\hat{\rho}_c = -\frac{\omega_c' eE_0}{\Omega md}\hat{z}\cos\omega_d t \ , \tag{32a}$$

$$\frac{d^2\hat{\rho}_m}{dt^2} + \omega_m^2\hat{\rho}_m = +\frac{\omega_m eE_0}{\Omega md}\hat{z}\cos\omega_d t \ , \tag{32b}$$

$$\frac{d^2\hat{z}}{dt^2} + \omega_z^2\hat{z} = -\frac{eE_0}{2md}(\hat{\rho}_c + \hat{\rho}_m)\cos\omega_d t \ . \tag{32c}$$

As before, we introduce slowly varying operators by defining $\hat{z} = \mathrm{Re}(\tilde{z}e^{i\omega_z t})$, $\hat{\rho}_c = \mathrm{Re}(\tilde{\rho}_c e^{i\omega_c' t})$, and $\hat{\rho}_m = \mathrm{Re}(\tilde{\rho}_m e^{-i\omega_m t})$. Parametric coupling of the axial and cyclotron motion occurs for $\omega_d = \omega_c' - \omega_z$. Substituting for ω_d, $\hat{z}$, $\hat{\rho}_c$, and $\hat{\rho}_m$ in Eqs. (32), and neglecting nonsecular terms, we find that

$$\frac{d\tilde{\rho}_c}{dt} = \frac{ieE_0}{4m\Omega d}\tilde{z} = \frac{ig_1^2}{4\omega_c'}\tilde{z} \ , \tag{33a}$$

$$\frac{d\tilde{z}}{dt} = \frac{ieE_0}{8m\omega_z d}\tilde{\rho}_c = \frac{ig_2^2}{4\omega_z}\tilde{\rho}_c \ , \tag{33b}$$

$$\frac{d\tilde{\rho}_m}{dt} = 0 \ . \tag{33c}$$

Equations (33a) and (33b) are of the form of Eqs. (24), with $\tilde{x}_1 \equiv \tilde{\rho}_c$, $\tilde{x}_2 \equiv \tilde{z}$, $\omega_1 \equiv \omega_c'$, $\omega_2 \equiv \omega_z$, $g_1^2 = \omega_c' eE_0/\Omega md$, and $g_2^2 = eE_0/2md$. Therefore the general solution is of the form of Eqs. (25), where $\hat{p}_1 = \hat{\pi}_c$, $\hat{p}_2 = \hat{p}_z$, $m_1 = m_2 = m$, $(\omega_2 g_1^2/\omega_1 g_2^2)^{1/2} = (2\omega_z/\Omega)^{1/2}$, and $\omega_{\text{ex}} = (eE_0/4md)(2\Omega\omega_z)^{-1/2}$. Again, the solution is exactly analogous to Eqs. (17), apart from the factor $(2\omega_z/\Omega)^{\pm 1/2}$ multiplying the $\sin\omega_{\text{ex}}t$ terms. Thus we find that for $t_{\text{ex}} = \pi/2\omega_{\text{ex}}$, the axial and cyclotron wave functions have exactly interchanged, apart from a phase shift of $\pi/2$. The factors $(2\omega_z/\Omega)^{\pm 1/2}$ normalize the wave functions, so that the number of quanta are conserved, and so that the exchanged wave functions have the same expansion in a basis of number states, apart from a phase shift.

A drive at $\omega_d = \omega_z + \omega_m$ will couple the axial and magnetron motions. The sum, rather than the difference, of the frequencies appears because of the inversion of the magnetron energy. By again substituting for ω_d, $\hat{\rho}_c$, $\hat{\rho}_m$,

and $\hat{z}$ in Eqs. (32) and neglecting nonsecular terms, we get

$$\frac{d\tilde{\rho}_c}{dt} = 0 \ . \tag{34a}$$

$$\frac{d\tilde{\rho}_m}{dt} = \frac{ieE_0}{4m\Omega d}\tilde{z} = \frac{ig_1^2}{4\omega_m}\tilde{z} \ , \tag{34b}$$

$$\frac{d\tilde{z}}{dt} = \frac{ieE_0}{8m\omega_z d}\tilde{\rho}_m = \frac{ig_2^2}{4\omega_z}\tilde{\rho}_m \ . \tag{34c}$$

In this case also, Eqs. (34b) and (34c) are of the form of Eqs. (24), with $\tilde{x}_1 \equiv \tilde{\rho}_m$, $\tilde{x}_2 \equiv \tilde{z}$, $\omega_1 \equiv \omega_m$, $\omega_2 \equiv \omega_z$, $g_1^2 = \omega_m eE_0/\Omega md$, and $g_2^2 = eE_0/2md$. The general solution is of the form of Eqs. (25), where $\hat{p}_1 = \hat{\pi}_m$, $\hat{p}_2 = \hat{p}_z$, $m_1 = m_2 = m$, $(\omega_2 g_1^2/\omega_1 g_2^2)^{1/2} = (2\omega_z/\Omega)^{1/2}$, $\omega_{\text{ex}} = (eE_0/4md)(2\Omega\omega_z)^{-1/2}$, and $\omega_1 \equiv -\omega_m$. Again, apart from a phase shift, the axial and magnetron wave functions are exchanged after a time $t_{\text{ex}} = \pi/2\omega_{\text{ex}}$, with the wave functions normalized so that the number of quanta are conserved.

The electron can be cooled into its $|n_z, n_c, n_m\rangle = |0,0,0\rangle$ ground state, by cooling to $n_z = 0$ via coupling to the ion, as illustrated in Fig. 4(a) and by then parametrically driving n_c to zero, recooling to $n_z = 0$ again, parametrically driving n_m to zero, and, finally, recooling n_z to zero. Measurements of the electron's cyclotron frequency may be carried out by first applying radiation with a frequency near ω_c' to drive the $|0,0,0\rangle$ to $|0,1,0\rangle$ transition, and then by parametrically exchanging the cyclotron and axial wave functions, as illustrated in Fig. 5. If no transition to the $|0,1,0\rangle$ state occurs after the radiation is applied, the final state of the electron after parametric exchange is $|0,0,0\rangle$; whereas, if a transition to $|0,1,0\rangle$ does occur, the final state of the electron is $|1,0,0\rangle$. The transition may be detected by detecting the presence of a quantum in n_z, by coupling to the ion, as illustrated in Fig. 4(b).

As discussed in Sec. III, the ability to cool and detect single-quantum excitations in this manner does not increase the inherent signal-to-noise ratio of the driven electron, given that a certain amount of damping is present and that a spectrally pure drive is available. Thus
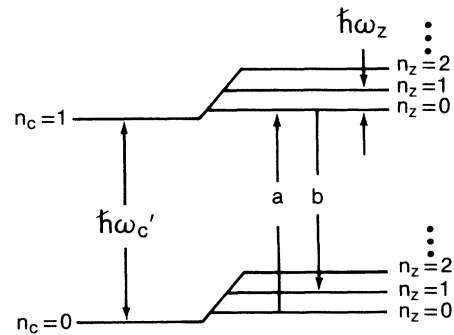

FIG. 5. Lowest electron cyclotron and axial energy levels, illustrating the transfer of a single cyclotron quantum into the axial motion. Only the few lowest cyclotron and axial levels are shown for clarity. (a) $|n_z, n_c\rangle = |0,0\rangle$ to $|0,1\rangle$ transition at ω_c'. (b) $|0,1\rangle$ to $|1,0\rangle$ transition at $\omega_c' - \omega_z$.

one can also achieve an equivalent signal-to-noise ratio by applying a strong continuous drive to the electron's motion, resulting in a large signal power, and by detecting the signal using conventional rf detection.[23] However, this introduces perturbations to the particle's frequencies ω_c', ω_z, and ω_m, making this large signal-to-noise ratio less useful to precision experiments.

For a purely quadratic electric potential and uniform magnetic field, the "true" cyclotron frequency of the particle, in terms of the *measured* frequencies ω_c', ω_z, and ω_m, is given by[23]

$$\omega_c^2 = (\omega_c')^2 + \omega_z^2 + \omega_m^2 .$$ (35)

This expression remains valid for arbitrary tilt angle of the magnetic field with respect to the trap axis.[23] The most important corrections to Eq. (35) arise from second-order inhomogeneities in the magnetic field, fourth-order corrections to the electric field, and relativistic corrections. (The magnetic- and electric-field inhomogeneities may be parametrized by coefficients B_2 and C_4, respectively.[23]) These corrections are proportional to the particle energies; so accuracy increases as the energies are lowered.

For trapped electron spectroscopy, the B_2 correction has typically been the largest, since a "magnetic bottle" (large B_2) has been deliberately applied for detection purposes.[23,27] However, it should be possible to reduce this, either by use of a "switchable bottle"[47] or by using alternative detection schemes without a magnetic bottle.[48] If such schemes are successful, the most important correction will be the relativistic shift $(\Delta\omega_c/\omega_c)_{rel} = -E_z/2mc^2$, where E_z is the axial energy. (We assume that the cyclotron motion has cooled to $\langle n_c \rangle < 1$ by cyclotron radiation, so that relativistic shift due to cyclotron motion may be precisely corrected for, as discussed below.) For $E_z = k_B T$, with $T = 4.2$ K, we find that $\Delta\omega/\omega_c = -3.5 \times 10^{-10}$. Thus electron-positron mass comparisons or g-factor anomaly measurements at or beyond a few parts in 10^{10} will require significantly lower axial temperatures. We note that presently the electron-positron mass ratio has been measured to one part in 10^7,[28] and their anomalies measured to two parts in 10^9.[27]

The character of the systematic corrections changes dramatically when the electron or proton can be cooled to its lowest quantum state. In this case, the resolved quantum level structure of the particle becomes apparent, as was illustrated in Fig. 5, and the perturbations take the form of energy-level shifts.[48] Also, since only single-quantum excitations are observed, the observed resonances will be sharp lines, not broadened by the perturbations. Since the relativistic level structure can be calculated with high precision, the "true" cyclotron frequency can be calculated from the observed level spacings, with well-known corrections taken into account. In fact, this quantum relativistic level structure is of interest in its own right. The relativistic corrections will therefore have essentially no effect on the measurement accuracy in the single-quantum regime.

One of the difficulties associated with mass comparisons[25-28] in the Penning trap is that the magnetic field typically drifts between the loading of one particle and the next. This has limited the accuracy of mass comparisons of atomic ions to a few parts in 10^{10}.[25,26] We envision performing such experiments with a single $^9Be^+$ ion as the detector ion (Appendices A and B). This nearby $^9Be^+$ ion can also serve as a highly accurate magnetometer by measurement of its ground-state electron spin-flip transition frequency, so that such drifts may be corrected for to a high degree. The B_2, C_4, and relativistic corrections are of comparable magnitudes for atomic ions and will limit accuracies to approximately one part in 10^{11} without improved cooling techniques. The present technique provides a means of dramatically lowering these corrections. Mass-ratio comparisons at or beyond a few parts in 10^{12} should be possible.

These techniques may be applied to a measurement of the electron g factor. In this case, the largest systematic effect has been a cavity shift of the cyclotron frequency.[23,49] The uncertainty in this effect could be substantially reduced, however, by choosing electrode shapes which approximate a cylindrical cavity.[49,50] Parameters could be chosen so that this cavity has a lowest-order mode frequency higher than the cyclotron frequency, so that the shift is much smaller and more tractable. The cavity shift effect is less important for the electron-positron g-factor ratio and mass ratio, since it should be the same for both particles. For the mass ratio, the limiting systematic error will most likely be due to an offset of the trap center for the electron compared with that for the positron, due to stray contact potentials. This causes the two particles to see a slightly different magnetic field.[51] We think that the techniques discussed here should allow improved electron-positron mass-ratio and g-factor comparisons. Similar improvements in accuracy should be possible for a direct measurement of the electron g factor, assuming that the cavity shift problem can be adequately addressed.

It should also be possible to make a high-precision measurement of the g factor of the isolated proton or other atomic ions. This measurement has not been carried out using existing techniques of single trapped-particle spectroscopy, because the proton spin and cyclotron magnetic moment are too small to detect the proton-spin flips with magnetic bottle techniques.[23] However, in the technique discussed here, the measurement sensitivity is great enough to detect the spin flips directly, as illustrated in Fig. 6. The proton can be prepared in the $|m_s = +\frac{1}{2}, n_c = 0 \rangle$ state by first preparing it in the $|\pm\frac{1}{2}, 0 \rangle$ state as described earlier, and parametrically driving at $\omega_s - \omega_c'$, where $\omega_s = g_p \mu_N B/\hbar$ is the spin-flip frequency, and μ_N is the nuclear magneton. The proton will either remain in the $|+\frac{1}{2}, 0 \rangle$ state or be driven to the $|+\frac{1}{2}, 1 \rangle$ state. The cyclotron quantum state is exchanged with the axial in an $|n_z = 0 \rangle$ state, as previously described, leaving the proton in the $|+\frac{1}{2}, 0 \rangle$ state. Spectroscopy of the spin-flip transition at ω_s is carried out by driving the $|+\frac{1}{2}, 0 \rangle \rightarrow |-\frac{1}{2}, 0 \rangle$ transition, followed by a drive at $\omega_s - \omega_c'$, transferring the proton to $|+\frac{1}{2}, 1 \rangle$ if a spin-flip transition occurs, or leaving it in $|+\frac{1}{2}, 0 \rangle$ if a transition does not occur. The cyclotron quantum is then detected
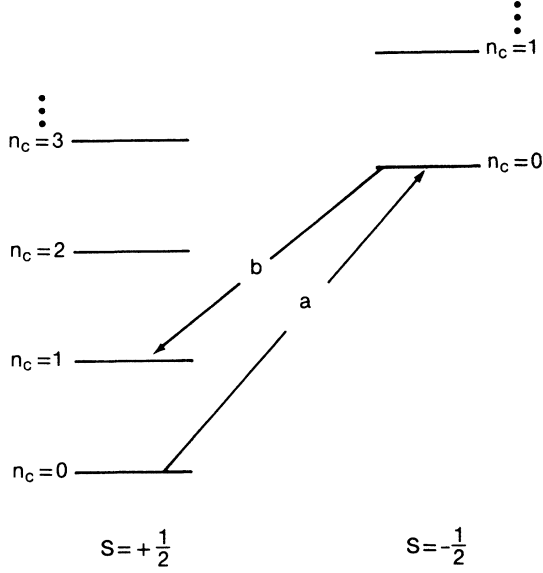
FIG. 6. Lowest proton cyclotron and spin energy levels, illustrating the transfer of proton spin-flip energy into the cyclotron motion. Only the few lowest cyclotron levels are shown for clarity. (a) $|+\frac{1}{2},0\rangle\to|-\frac{1}{2},0\rangle$ spin-flip transition at ω_s. (b) $|-\frac{1}{2},0\rangle\to|+\frac{1}{2},1\rangle$ transition at $\omega_s-\omega_c'$.

as described in Fig. 5. In this way, single-quantum spin-flip transitions may be detected and the proton g factor determined by $g_p=2\omega_s/\omega_c$.

The proton g factor enters into the determination of the fundamental constants via the three quantities $g_p/2=\mu_p/\mu_N$, μ_p/μ_B, and m_p/m_e. The two most precisely measured of these quantities determine the third and also appear as auxiliary constants in the least-squares adjustment of the fundamental constants.[52] At present, μ_p/μ_B and m_p/m_e are the most precisely determined, with fractional uncertainties 1×10^{-8} and 2×10^{-8}, respectively.[52] All three of these quantities might be measured with improved accuracy by the techniques discussed here. Also, the proton-antiproton g-factor ratio might be measured with these techniques.

VI. SQUEEZING AND SIGNAL DETECTION BY PARAMETRIC AMPLIFICATION

We have so far described only measurement by quantum multiplication. Linear amplification using a single stored ion is also possible: Degenerate parametric amplification occurs if the ion trap's ring-end-cap voltage is driven at twice the ion's axial resonance frequency.[53] This process can amplify one of the oscillator's two quadrature components with no added noise.[4] The quadrature components $\hat{X}_1$ and $\hat{X}_2$ are defined by[4,30]

$$\hat{a}=(\hat{X}_1+i\hat{X}_2)e^{-i\omega t} , \qquad (36a)$$

$$\hat{a}^\dagger=(\hat{X}_1-i\hat{X}_2)e^{+i\omega t} . \qquad (36b)$$

In terms of $\hat{X}_1$ and $\hat{X}_2$, the displacement operator $\hat{z}$ may be written as

$$\hat{z}=\left[\frac{2\hbar}{m\omega}\right]^{1/2}(\hat{X}_1\cos\omega t+\hat{X}_2\sin\omega t) , \qquad (37)$$

so that $\hat{X}_1$ and $\hat{X}_2$ may be identified with the $\cos\omega t$ and $\sin\omega t$ components of the oscillation. $\hat{X}_1$ and $\hat{X}_2$ satisfy the uncertainty relation

$$\Delta\hat{X}_1\Delta\hat{X}_2\geq\tfrac{1}{4} , \qquad (38)$$

where $\Delta\hat{X}_i\equiv\langle(\Delta\hat{X}_i)^2\rangle^{1/2}$ is the rms fluctuation of $\hat{X}_i$ about its mean. For the vacuum state or for a coherent state, $\Delta\hat{X}_1$ and $\Delta\hat{X}_2$ are equal: $\Delta\hat{X}_1=\Delta\hat{X}_2=\tfrac{1}{2}$.

Consider the state in which the operators have initial value $\hat{X}_1(t_1)$ and $\hat{X}_2(t_1)$ at time $t=t_1$. Degenerate parametric amplification of this state occurs when an oscillating potential $\text{Re}(Ve^{2i\omega t})$ is applied between the ring and end-cap electrodes of the ion trap, with V a complex constant, $V=|V|e^{i\theta}$. This gives rise to an added potential

$$\phi=\frac{r^2-2z^2}{d_T^2}\text{Re}(Ve^{2i\omega t}) , \qquad (39)$$

where d_T is a characteristic trap dimension. The Hamiltonian describing the axial motion of the ion then becomes

$$H=\hbar\omega(\hat{a}^\dagger\hat{a}+\tfrac{1}{2})-\frac{2e\hat{z}^2}{d_T^2}\text{Re}(Ve^{2i\omega t}) . \qquad (40)$$

Neglecting nonsecular terms the Heisenberg equations of motion for $\hat{X}_1$ and $\hat{X}_2$ become

$$\frac{d\hat{X}_1}{dt}=\xi(\hat{X}_2\cos\theta+\hat{X}_1\sin\theta) , \qquad (41a)$$

$$\frac{d\hat{X}_2}{dt}=\xi(\hat{X}_1\cos\theta-\hat{X}_2\sin\theta) , \qquad (41b)$$

where $\xi=e|V|/md_T^2\omega$. For $\theta=\pi/2$, Eqs. (41) have the solution

$$\hat{X}_1(t_2)=G^{1/2}\hat{X}_1(t_1) , \qquad (42a)$$

$$\hat{X}_2(t_2)=G^{-1/2}\hat{X}_2(t_1) , \qquad (42b)$$

with $G=\exp[2\xi(t_2-t_1)]$. Thus the component $\hat{X}_1$ is amplified by the factor $G^{1/2}$; $\hat{X}_2$ is attenuated by the same factor. Similarly, for $\theta=-\pi/2$, $\hat{X}_2$ is amplified and $\hat{X}_1$ attenuated.

Suppose that a signal X_{1s}, which results from a drive applied from time $t=0$ to t_1, is present in $\hat{X}_1$. We have

$$\hat{X}_1(t_1)=\hat{X}_1(0)+X_{1s} . \qquad (43)$$

This equation follows from Eq. (8) and the corresponding conjugate equation for $a^\dagger(t_1)$, where $X_{1s}=(f_{s0}+f_{s0}^*)t_1/2$, with $f=f_{s0}e^{-i\omega t}$, and where we assume that $\gamma t_1\ll1$ and that the noise term may be neglected. $\hat{X}_1(t_1)$ may be amplified according to Eqs. (42), giving a signal S and noise N of

$$S=\langle\hat{X}_1(t_2)\rangle^2=GX_{1s}^2 , \qquad (44)$$

$$N=\langle\Delta\hat{X}_1(t_2)^2\rangle=G\langle\Delta\hat{X}_1(0)^2\rangle , \qquad (45)$$

where we assume that $\langle\hat{X}_1(0)\rangle=0$. For G sufficiently

large, S can be detected with negligible additional noise by monitoring changes in the laser-induced fluorescence of the ion[24] or by detecting the ion's image current with conventional electronics. (For example, in the work of Refs. 26 and 46, the axial amplitudes of single ions are determined with a signal-to-noise ratio greater than unity in a single measurement.) The resulting signal-to-noise ratio S/N is just that of the state before amplification. For an initial vacuum state at $t=0$, $\langle \Delta \hat{X}_1(0)^2 \rangle = \frac{1}{4}$, which gives $S/N = 4X_{1s}^2$.

The fluctuations in the signal quadrature $\hat{X}_1$ may be reduced at the expense of increased fluctuations in quadrature $\hat{X}_2$, by preparing the oscillator in a squeezed state.[4,30] Such a state may be characterized by a wave function (at $t=0$) given by[31]

$$\psi_{sq}(z) = N_{sq} e^{(-1/2)[\beta(m\omega/\hbar)z^2 - 2\beta\delta(2m\omega/\hbar)^{1/2}z]} . \quad (46)$$

Here β is the "squeeze parameter," δ is a coherent amplitude in the $\hat{X}_1$ quadrature and N_{sq} is a normalization factor.

In this state, the variance of $\hat{X}_1$ is decreased by the factor β. Thus the noise is $N_s = 1/4\beta$, and the signal-to-noise ratio $S/N_s = 4\beta X_{1s}^2$, an improvement by the factor β. For $\beta \gg 1$, this implies that a signal energy $\hbar\omega/\beta$, which contains much less than one quantum, may be detected with a signal-to-noise ratio of order unity in a single measurement. Therefore signal detection by degenerate parametric amplification is in principle more sensitive than signal detection by direct measurement of absorbed quanta.

A very direct method of producing the state given by Eq. (46), illustrated in Fig. 7, is to first prepare the ion in the ground state ψ_0' of a well with a different restoring potential $\phi'(z') = m(\omega')^2(z')^2/2q$ $(\omega' > \omega)$ and different origin $\Delta = z - z'$, and then nonadiabatically dropping the potential back to $\phi(z) = m\omega^2 z^2/2q$.[32] This produces the squeezed state

$$\psi_0'(z') = \frac{1}{\pi^{1/4}} e^{(-1/2)(m\omega'/\hbar)(z-\Delta)^2} = \psi_{sq}(z) . \quad (47)$$

This implies that $\beta = \omega'/\omega$, and that $\delta = \Delta(m\omega/2\hbar)^{1/2}$.

A second method of preparing an initially squeezed state is to prepare an initial vacuum state, followed by a parametric drive as in Eqs. (41), with $\theta = -\pi/2$. The variance in the $\hat{X}_1$ quadrature is reduced by a factor G, while that in the $\hat{X}_2$ quadrature is increased by the factor G. The wave function is of the form of Eq. (46) with $\delta = 0$ and $\beta = G$.

Squeezing and detection by degenerate parametric amplification may be extended to source oscillators other than the ion by the methods described in Sec. III. Thus, if the ion is prepared in an initially squeezed state and coupled to a source oscillator as in Fig. 3, after a time t_{ex}, the oscillators have exchanged wave functions; so the source oscillator is prepared in a squeezed state. A signal drive applied to the source generates a source excitation analogous to that described by Eq. (43). The squeezed and driven source oscillator wave function may then be transferred back to the ion, and its $\hat{X}_1$ quadrature amplitude measured by degenerate parametric amplification of
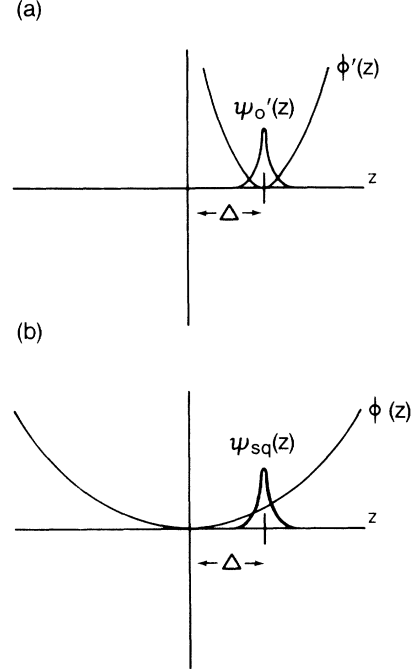

FIG. 7. Preparation of a squeezed state by a nonadiabatic change in the trapping potential. (a) Potential and wave function immediately preceding the potential change where the ion is assumed to be cooled into its ground state of the potential well represented by $\phi'(z)$. (b) Restored potential and squeezed wave function immediately after changing the potential from $\phi'(z)$ to $\phi(z)$.

the ion's axial motion. In an experiment to measure a very weak force by its excitation of a high-Q oscillator, both quadrature amplitudes may be measured with high sensitivity by using two oscillators, one for each quadrature.[54]

The buildup of thermal excitation in an oscillator is described by Eq. (9). For $\gamma t_1 \ll 1$, it follows from Eq. (9) and its conjugate that there is a contribution to the variance $\langle \Delta X_1(t_1)^2 \rangle$ of $\gamma(\bar{n} + \frac{1}{2})t_1/2$. Thus, if thermal noise introduced by the coupling of the oscillator to a thermal reservoir is to be negligible, we require $\gamma(\bar{n} + \frac{1}{2})t_1/2 \ll \langle \Delta X_1(0)^2 \rangle = 1/4\beta$. For $\beta = 1$ (no squeezing), this is essentially the same requirement on oscillator Q as the inequality (21); for $\beta > 1$, the oscillator's Q must be still higher by a factor of β.

VII. CONCLUSION

Sensitive detection of signals requires that both signal source and detector exhibit low damping rates, that the source and detector couple efficiently, and that some means is available to cool both source and detector to a temperature of order $\hbar\omega/k_B$. In addition, the detector should provide nearly quantum-limited gain. We have shown that a single laser-cooled trapped ion, coupled to a high-Q source through image currents in the trap electrodes, can provide a realization of such high-sensitivity detection in the rf regime.

Such a detector may have important applications to

precision measurement. We have analyzed one application, the cooling and detection of motions of a second trapped charged particle, and seen that improved accuracy and sensitivity may be expected. These techniques may improve the accuracy of measurements of the electron g factor,[27] electron-positron g-factor ratio,[27] and mass ratio,[28] and can in principle yield the proton g factor and the proton-antiproton mass ratio[29] and g-factor ratio. By extension, these techniques may also find application to measurement of mass or internal degrees of freedom of other atomic or molecular ions. These methods may also prove useful in any experiment requiring very high sensitivity in the rf range or at lower frequencies, such as in gravity wave detection, or detection of very weak forces.[15-18]

Because this kind of experiment is conceptually simple, it may prove useful as a testing ground for topics in quantum measurement theory. For example, studies of squeezed states or quantum limits to signal detection may be carried out this way. The quantum behavior of single trapped particles may also be studied.

An important question is how practical the proposed methods are. This has already been demonstrated to some degree in Ref. 14, and in Appendices A–C we further examine the experimental possibilities. We are currently developing a coupled-trap experiment similar to that described in Appendix B.

ACKNOWLEDGMENTS

APPENDIX A: RAMAN SIDEBAND COOLING AND DETECTION

Most of the experimental techniques discussed in this paper depend on resolved sideband cooling and detection. As described in Sec. II, this requires an ion with the level structure shown in Fig. 2, with easily accessible "weak" ($\gamma_w \ll \omega_z$) and "strong" transitions. Since typically $\omega_z \simeq 1$ MHz, this condition is so far experimentally satisfied only in a few relatively heavy ions, such as Hg^+ (Refs. 14, 32, and 43) or Ba^+ (Refs. 41 and 44) where optical transitions to metastable levels occur. A technique to cool lighter ions is desirable, since this maximizes the coupling between the ion and source.

In this section, we describe how a stimulated Raman transition between two ground-state sublevels (or a ground state and metastable excited state) may serve as the "weak" transition. In this way, sideband cooling may be extended to lighter ions, such as $^9Be^+$, which is the lightest ion which can easily be laser cooled by Doppler cooling.[55,56] Cooling by stimulated Raman transitions has been previously discussed for the case of Ba^+.[57,58]

The general principle of Raman sideband cooling for the axial energy of the ion is illustrated in Fig. 8. We
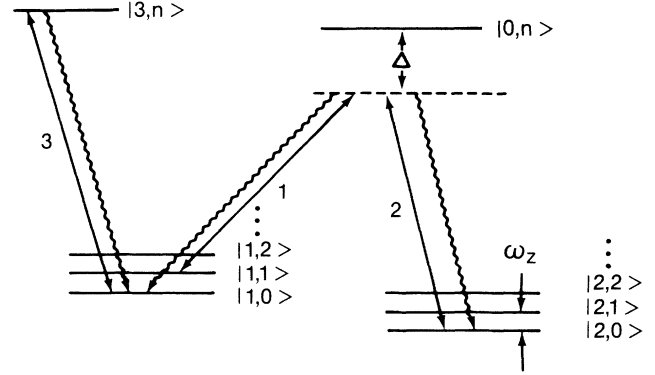

FIG. 8. Energy-level structure for Raman sideband cooling and detection. The Raman cooling transitions are induced by beams 1 and 2; beam 3 is used only for detection of Raman cooling and for Doppler precooling.

consider a four-level system with lower levels $|1\rangle$ and $|2\rangle$ coupled to a common upper level $|0\rangle$. We also assume that level $|1\rangle$ is coupled to an upper level $|3\rangle$, which decays only back to level $|1\rangle$. The $|1\rangle \rightarrow |3\rangle$ transition will serve as the detector of Raman cooling and will also provide Doppler precooling. We denote the combined internal-translational states by $|J,n\rangle$, where J denotes the internal state ($J = 0, \ldots, 3$) and n the axial harmonic oscillator quantum number. Two classical fields,

$$\mathbf{E}_J = \mathrm{Re}(\mathbf{E}_{0J} e^{i(\mathbf{k}_J \cdot \mathbf{r} - \omega_J t)}), \quad J = 1,2 , \tag{A1}$$

couple level $|0\rangle$ to levels $|1\rangle$ and $|2\rangle$, with Rabi frequencies $g_{0J} = |\boldsymbol{\mu}_{0J} \cdot \mathbf{E}_{0J}|/2\hbar$, where $\mu_{0J} = \langle 0|\mu|J\rangle$ is the dipole matrix element between states $|0\rangle$ and $|J\rangle$ ($J = 1,2$). The frequencies of the two beams are assumed to be equal to

$$\omega_1 = \omega_{01} - \Delta - \omega_z , \tag{A2a}$$

$$\omega_2 = \omega_{02} - \Delta , \tag{A2b}$$

where ω_{0J} is the transition frequency between states $|0,n\rangle$ and $|J,n\rangle$, and ω_z is the axial oscillation frequency of the ion.

The difference frequency $\omega_1 - \omega_2$ is tuned to the first lower sideband of the $|1\rangle \leftrightarrow |2\rangle$ stimulated Raman transition, inducing primarily $|1,n\rangle \leftrightarrow |2,n-1\rangle$ transitions. For effective cooling, we require that

$$\beta_J = \frac{R_J}{\hbar\omega_z} \ll 1 , \tag{A3}$$

where $R_J = (\hbar k_J)^2/2m$ is the recoil energy for the $|0\rangle \rightarrow |J\rangle$ transition ($J = 1,2$). In addition, spontaneous Raman scattering occurs. When $\beta \ll 1$, spontaneous scattering occurs predominantly with $\Delta n = 0$. Thus cooling can occur by means of stimulated Raman transitions $|1,n\rangle \rightarrow |2,n-1\rangle$, followed by spontaneous Raman transitions $|2,n-1\rangle \rightarrow |1,n-1\rangle$.[57] In this case, cooling by stimulated Raman transitions is essentially the same as laser cooling using a narrow optical transition, as illustrated in Fig. 2. In the case of Fig. 2, there is no intermediate level, and the $|J=2\rangle$ level of Fig. 8 is replaced

by the $|w\rangle$ level of Fig. 2. In the case of Fig. 2, the atom is recycled back to the ground state by spontaneous emission $|w\rangle \rightarrow |g\rangle$, rather than by spontaneous Raman transitions $|2,n\rangle \rightarrow |0,n\rangle \rightarrow |1,n\rangle$.

A quantitative description of this cooling process is fairly complex and requires a solution of the density matrix equations for the infinite ladders of states $|J,n\rangle$, $J = 0, \ldots, 3$; $n = 0, \ldots, \infty$. In order for efficient cooling to occur, the atom must make the $|1\rangle \rightarrow |2\rangle$ transition primarily by stimulated Raman scattering, and the $|2\rangle \rightarrow |1\rangle$ transition primarily by spontaneous Raman scattering. One means of accomplishing this with cw excitation is to make $g_{02} \gg g_{01}$.[57] This case has been analyzed by Lindberg and Javanainen,[59] who obtain limiting values of the temperature. In this section, we discuss an alternative method, based on Raman excitation in the transient regime. The analysis of this method is somewhat simpler than the cw case. In addition, this method provides an efficient means of detecting the final temperature.

We first suppose the ion is in the level $|1,n\rangle$, and that both beams are turned on for a time t, where t is sufficiently small that the probability of a spontaneous transition is small. The behavior of the system is adequately described by amplitude equations,

$$\frac{da_{Jn}}{dt} = \frac{-i}{\hbar} \sum_{J',n'} a_{J'n'} e^{i\omega_{JnJ'n'}t} V_{JnJ'n'} - \frac{\gamma_J}{2} a_{Jn} . \quad \text{(A4)}$$

In Eq. (A4), a_{Jn} is the amplitude for the state $|J,n\rangle$, $\hbar\omega_{JnJ'n'}$ is the energy of state $|Jn\rangle$ minus the energy of $|J'n'\rangle$, $V_{JnJ'n'}$ is the matrix element of the perturbation $-\boldsymbol{\mu}\cdot(\mathbf{E}_1+\mathbf{E}_2)$ between states $|J,n\rangle$ and $|J'n'\rangle$, and $\gamma_J = \gamma\delta_{J0}$, where γ is the total spontaneous decay rate of level 0.

If the condition (A3) is satisfied, if $k_J z_0 n^{1/2} \ll 1$, and if

$$|g_{01}| = |g_{02}| \equiv g , \quad \text{(A5a)}$$

$$\Delta \gg \frac{\pi\gamma}{2|\delta k_z|z_0 n^{1/2}} , \quad \text{(A5b)}$$

$$\frac{g^2}{\Delta} \ll \omega_z , \quad \text{(A5c)}$$

then we can show from Eqs. (A4) that for times $t \lesssim 1/\Omega$ only the $|1,n\rangle \leftrightarrow |2,n-1\rangle$ transition is appreciably excited, and that the populations of these two levels are given approximately by

$$P_{1,n} \simeq \cos^2\Omega t , \quad \text{(A6a)}$$

$$P_{2,n-1} \simeq \sin^2\Omega t , \quad \text{(A6b)}$$

where

$$\Omega = \frac{g^2}{\Delta}|\delta k_z|z_0 n^{1/2} . \quad \text{(A7)}$$

Here $\delta k_z = k_{2z} - k_{1z}$ is the difference between the z components of the wave vectors of beams 2 and 1, and $z_0 = (\hbar/2m\omega_z)^{1/2}$ is the spread of the zero-point motion of the ion in the axial well. We see that a kind of coherent "Rabi oscillation" between the two lower levels

is observed, and that, if the two beams are left on for a time $t_\pi = \pi/2\Omega$, a "Raman π pulse" is obtained, in which the population of level $|1,n\rangle$ is completely transferred to $|2,n-1\rangle$.

The first inequality (A5b) guarantees that the total spontaneous decay probability out of level $|0\rangle$ is small, and the second inequality (A5c) guarantees that the population transferred by stimulated Raman transitions to states other than $|2,n-1\rangle$ state is small. This "Rabi oscillation" is similar to that which has been previously analyzed for a three-level system;[60] our analysis differs in that a minimum of four levels is involved, since the Raman transition proceeds equally through the two excited levels $|0,n\rangle$ and $|0,n-1\rangle$. If $|g_{01}| \neq |g_{02}|$, a coherent population exchange still occurs but with less than 100% efficiency (similar to the three-level case[60]).

The behavior given by Eqs. (A6) indicates that the Raman transition may be used to verify that the ion has been cooled into the state $|1,n\rangle$, with $\langle n \rangle \ll 1$. The two laser beams are pulsed on for a time t_π corresponding to $n = 1$. The ion is transferred to the $|2,0\rangle$ state with high probability if it was initially in $|1,1\rangle$; but if it was initially in the state $|1,0\rangle$, it remains there. This behavior is illustrated in Fig. 9, which shows the result of a numerical
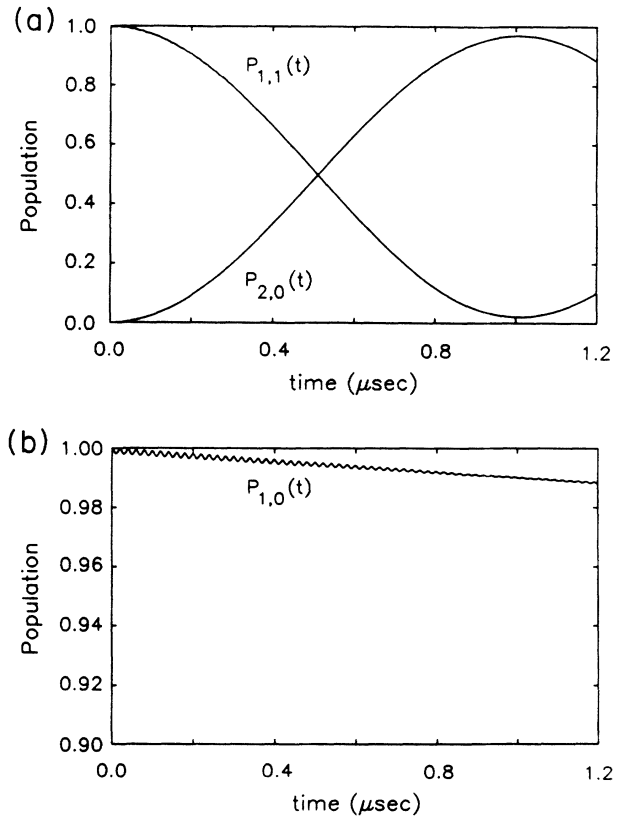

FIG. 9. Level populations for stimulated Raman transitions as functions of time of the states $|J,n\rangle$. Parameters are $|g_{01}|/2\pi = |g_{02}|/2\pi = 40$ MHz, $\Delta/2\pi = 1.5$ GHz, $\omega_z/2\pi = 5$ MHz, and $k_{1z}z_0 = -k_{2z}z_0 = 0.115$. (a) Populations of the $|1,1\rangle$ and $|2,0\rangle$ states, with all population initially in the $|1,1\rangle$ state. (b) Population of the $|1,0\rangle$ state, with all population initially in the $|1,0\rangle$ state.

integration of Eq. (A4). In this simulation, couplings are considered only up to the first order in $k_J z_0 n^{1/2}$, and the basis includes only the $n = 0$, 1, and 2 levels of each electronic state. For the parameters indicated in Fig. 9, the $|1,1\rangle \rightarrow |2,0\rangle$ transition is driven with over 97% probability, whereas transitions out of the $|1,0\rangle$ state occur with less than 1% probability. The amplitude equations do not include the repopulation of the ground states due to spontaneous emission from the excited states. For the conditions of Fig. 9, (a) and (b), the integrated decay probability during the time t_π is $(g/\Delta)^2 \gamma t_\pi \approx 0.9\%$. Thus, for the conditions of Fig. 9(b), most of the population loss from the $|1,0\rangle$ state occurs via spontaneous emission, and most of this population returns to the $|1,0\rangle$ state by the end of a cooling cycle, since the probability for the ion to recoil into the $n = 1$ state for a single spontaneous scattering event is $\approx \beta \ll 1$ (see discussion below). The presence or absence of the initial $n = 1$ quanta may be determined by following the Raman pulse with a pulse of radiation on the $|1\rangle \leftrightarrow |3\rangle$ transition, which here plays the role of the strong transition in a manner analogous to that discussed in Sec. II.

Equations (A6) also suggest one means of cooling the ion. The ion is first precooled by ordinary Doppler cooling[55,56] on the $|1\rangle \rightarrow |3\rangle$ transition to a condition where $\langle n \rangle = n_D = (\gamma_3/\omega_z - 1)/2$.[37] Beams 1 and 2 illuminate the ion, with $|g_{01}| = |g_{02}|$, and beam 1 is chopped on and off, with the initial "on" period adjusted to give a "π pulse" with $n = 1$, and the "off" period sufficiently long that the ion returns from state $|2\rangle$ to state $|1\rangle$ by spontaneous Raman scattering with high probability. The ion then is pumped down the ladder of states, losing, on average, approximately one quantum per on-off cycle. (Ramping the pulse length from $t_\pi n_D^{-1/2}$ to t_π would shorten the cooling time.) This may or may not be more efficient than a scheme in which both lasers are left on continuously with $|g_{02}| \gg |g_{01}|$; it has the advantage that the experiment will already be set up in this way for detection purposes, and that the cooling time may readily be estimated. The limiting population of the $n = 1$ state will be determined by the probability that an ion in the $|1,0\rangle$ level is promoted into the $|1,1\rangle$ level during one cooling cycle. This can occur by an off-resonant stimulated Raman transition with probability of order $P_{\text{st.R}} = (g^2/\Delta\omega_z)^2$. Also, the ion can reach the $|1,1\rangle$ state by spontaneous Raman transitions, either by directly undergoing the $|1,0\rangle \rightarrow |1,1\rangle$ transition, or by first undergoing the $|1,0\rangle \rightarrow |2,0$ or $1\rangle$ transition during the beam 1 on period, and then the $|2,0$ or $1\rangle \rightarrow |1,1\rangle$ transition during the beam 1 off period. Both of these processes occur with a probability of order $P_{\text{sp.R}} = (g/\Delta)^2 \gamma \beta t_\pi$. An ion reaching the $|1,1\rangle$ level returns to the $|1,0\rangle$ level during the following cooling cycle with high probability. Therefore the average population of the $|1,1\rangle$ level is approximately given by the greater of $P_{\text{st.R}}$ or $P_{\text{sp.R}}$. For the example of Fig. 9, $P_{\text{st.R}} = 4.6 \times 10^{-4}$ and $P_{\text{sp.R}} = 3.9 \times 10^{-4}$; so the limiting population of the $n = 1$ state is $\sim 10^{-3}$.

In addition to cooling the axial motion, the particle's two transverse degrees of freedom will heat because of recoil. This will not affect the present discussion as long as the transverse motion is not inordinately hot, since the Raman transitions are sensitive only to axial temperature if $\mathbf{k}_1 - \mathbf{k}_2$ is oriented along $\hat{z}$. The transverse temperature may be kept reasonably low by periodic application of Doppler cooling by beam 3, presumably during detection periods. Also, the sideband cooling methods discussed here may easily be extended to the particle's transverse degrees of freedom, so that a very low temperature in three dimensions may be obtained.

The Raman sideband cooling method discussed here may be implemented in the $^9\text{Be}^+$ ion.[20] We assume that the $^9\text{Be}^+$ ion Zeeman sublevels are split by a strong magnetic field, and that the hyperfine structure may be neglected due to optical pumping[61] into the nuclear spin state $m_I = +\frac{3}{2}$. The levels corresponding to Fig. 8 are

$$|1\rangle \equiv |^2S_{1/2}, m_J = +\tfrac{1}{2}\rangle \ ,$$

$$|2\rangle \equiv |^2S_{1/2}, m_J = -\tfrac{1}{2}\rangle \ ,$$

$$|0\rangle \equiv |^2P_{3/2}, m_J = +\tfrac{1}{2}\rangle \ ,$$

$$|3\rangle \equiv |^2P_{3/2}, m_J = +\tfrac{3}{2}\rangle \ .$$

The parameters given in Fig. 9 are representative of those which may be obtained with $^9\text{Be}^+$ in a Penning trap with a large magnetic field ~ 6 T. For these conditions, $n_D = 2.4$; so only a few Raman cooling cycles are necessary to obtain $\langle n \rangle \ll 1$.

APPENDIX B: EXAMPLE DESIGN PARAMETERS FOR A COUPLED-TRAP EXPERIMENT

In this section we discuss the design of an experiment to cool and detect excitations of an electron in a Penning trap. We assume that a $^9\text{Be}^+$ ion is cooled and detected by the Raman sideband method discussed in Appendix A. The electron is assumed to be confined in a Penning trap of end-cap separation d_e, and the ion in a second Penning trap of end-cap separation d_i. We assume that the two traps are arranged in a coaxial fashion, as illustrated in Fig. 10, with a common central end-cap elec-
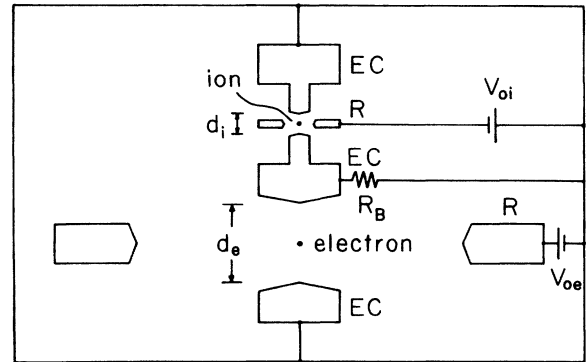

FIG. 10. Coupled-trap experiment: End-cap electrode (EC) and ring electrode (R). The central end cap is common to the two traps and is connected to the shield by resistor R_B. The trap electrodes and shield (outer boundary) are drawn to scale, with $d_e = 0.4$ cm, and are assumed to have cylindrical symmetry.

trode, and with the two remaining end-cap electrodes connected to an outer conducting shield. The central electrode may be connected to the shield potential via a large resistor and small shunt capacitance, without introducing significant thermal noise or excess capacitance. Potential differences of V_{0e} and V_{0i} are applied between the shield and the electron trap and ion trap ring electrodes, respectively.

We have evaluated the trap design in Fig. 10 numerically, using a modified version of the computer code POISSON.[62] Figure 10 is drawn to scale, and we assume that $d_e = 0.4$ cm $(d_i = 0.1$ cm). We assume that the trap capacitance C_T is given by its upper limit, which is simply the sum of the capacitances of the central end-cap electrode to all other electrodes and to the shield. We find that

$$C_T \simeq 0.30 \text{ pF} , \tag{B1}$$

$$l_e = m_e (d_e / \alpha_e e)^2 = 905 \text{ H} , \tag{B2}$$

$$l_i = m_i (d_i / \alpha_i e)^2 = 9.86 \times 10^5 \text{ H} , \tag{B3}$$

where we calculate that $\alpha_e = 0.793$, and $\alpha_i = 0.772$. If the traps are placed in a magnetic field of 6 T, then the ^{9}Be$^+$ cyclotron frequency ν_c is 10.2 MHz, and the maximum axial frequency is $\nu_z(\text{max}) = \nu_c / 2^{1/2} = 7.23$ MHz. We assume that $\nu_z = 5$ MHz, which then gives

$$t_{ex} = 2\pi^2 \nu_z (l_e l_i)^{1/2} C_T = 0.88 \text{ s} , \tag{B4}$$

Finally, we calculate that the axial potentials of the two traps are given by

$$V_e(z_e) = 0.563 (z_e / d_e)^2 V_{0e} , \tag{B5}$$

$$V_i(z_i) = 1.82 (z_i / d_i)^2 V_{0i} , \tag{B6}$$

where z_e and z_i are the electron's and ion's axial displacements from the center of their traps. This implies that an axial oscillation frequency of $\nu_z = 5$ MHz is obtained in each trap for $V_{0e} = 79.8$ mV, and $V_{0i} = 25.5$ V.

The time t_{ex} must be shorter than the time for absorption of one thermal quantum of energy on the axial motion of either the ion or the electron. This seems feasible, since a heating rate of approximately six quanta/s was obtained in the Hg$^+$ experiments,[14] and this may presumably be improved upon. For single-quantum excitation and detection of the electron's other degrees of freedom, the excitation of that degree of freedom and transfer into the axial motion must be shorter than the time for single-quantum excitation on that degree of freedom due to thermal radiation. The traps must be harmonic and tuned into resonance with each other to an accuracy better than $\Delta \nu_z \simeq 1/2t_{ex} = 0.57$ Hz, or a relative accuracy better than 1.1×10^{-7}. This may be difficult but also seems feasible.

APPENDIX C: CONTINUOUS REFRIGERATION

The previous discussions have concentrated on cooling the source modes to the zero-point energy. For some applications, this degree of cooling may not be required and a more modest form of the basic scheme can be em-

ployed.

As an example, consider that a cloud of N trapped ions which is laser cooled is used as a refrigerator. For simplicity, we assume that the cooling transition's radiative decay rate γ is larger than the ion's motional frequencies; that is, we are in the Doppler-cooling regime.[55,56] We will consider, as before, the axial motion of the ions, but similar arguments apply to the other degrees of freedom. For this case, Fig. 11 applies where we can determine R_N from the following argument. Near the Doppler-cooling limit, the cooling rate is approximately [see, for example, Eq. (10) of Ref. 39]

$$\frac{dE_z}{dt} = \frac{I\sigma_0}{\hbar \omega_L} R \left[-\frac{2E_z}{\hbar \gamma} + 1 \right] , \tag{C1}$$

where I is the laser beam intensity on the ions, σ_0 is the resonant scattering cross section, ω_L is the laser frequency, E_z is the total axial energy, and I is assumed to be below saturation. We assume that the recoil energy R is such that $R \ll \hbar \gamma$, and that the laser is tuned to $\omega_0 - \omega_L \simeq \gamma / 2$ for minimum temperature, where ω_0 is the rest frequency of the cooling transition. Equation (C1) applies as long as the Doppler width of the cooling transition is less than the natural width γ. Equation (C1) can be rewritten

$$\frac{d}{dt}(E_z - \hbar \gamma / 2) = -\dot{N}_s \frac{2R}{\hbar \gamma}(E_z - \hbar \gamma / 2) , \tag{C2}$$

where $\dot{N}_s = I\sigma_0 \hbar \omega_L$ is the resonant scatter rate. ($\dot{N}_s < \gamma$ by the assumption that the laser intensity is below saturation.) The energy decay rate for the equivalent circuit in the left-hand side of Fig. 11 is equal to R_N / l_N; so we make the identification that laser cooling can be represented by a resistor R_N at temperature T_N, where

$$R_N = l_N \dot{N}_s R / (\hbar \gamma / 2) , \tag{C3}$$

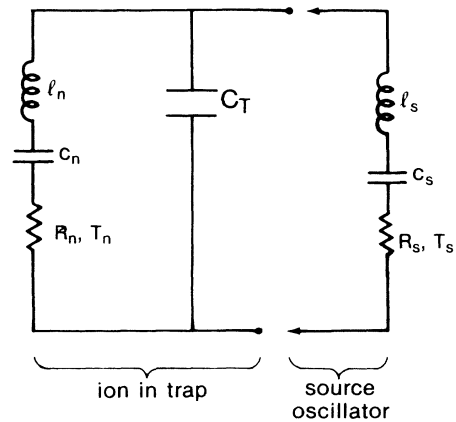and where[34] $l_N = l_i / N$, l_i is given in Eq. (2a), and

FIG. 11. Use of a cloud of N ions $(l_n = l_i / N)$ as a continuous refrigerator to cool a source mode represented by a series $L_s C_s R_s$ circuit. The resulting source "temperature" T_s^* is assumed to be given by $\langle i_s^2 \rangle l_s / k_B$, where i_s is the total rms current in the inductor l_s.

$T_N = \hbar\gamma/2k_B$ is the Doppler-cooling limit.[55,56] For laser-cooled Be^+ ions as the refrigerator, $\gamma/2\pi = 19.4$ MHz assuming laser cooling on the 313-nm first resonance line. Then $R_N \simeq 2.2 \times 10^4 [\dot{N}_s(s^{-1})/N]$ Ω. Since $\dot{N}_s$ can be as high as approximately $10^8/s$, extremely large values of resistance at the Doppler-cooling-limit temperature $[T_N(Be^+) \simeq 0.5$ mK$]$ can be obtained.

The main problem in achieving strong damping of source modes is the shunting effect of the trap capacitance C_T. This is not a problem as long as the coupling of the source oscillator mode to external heat sources is weak $(R_s \rightarrow 0)$, in which case the source mode comes to the temperature T_N of the cooled ion. This would be a good approximation in the example where the axial motion of an electron is cooled by the axial motion of an ion (Appendix B). In principle, the shunting effects of the trap capacitance can be eliminated by using an inductor in parallel with the trap capacitance. This might be used to advantage in some cases, but the heating effects due to losses in this inductor may outweigh the benefits of the capacitance cancellation.

The refrigerator ions can also be used to cool a mode of a macroscopic oscillator such as a quartz crystal. The equivalent circuit of a quartz-crystal resonator is essentially the same as that of ions in the trap; that is, a series

$L_Q R_Q C_Q$ circuit in parallel with electrode capacitance C_0. To get an idea of the degree of cooling that could be obtained, assume[63] that $L_Q = 19.5$ H, $R_Q = 65$ Ω, $(L_Q C_Q)^{-1/2} = 2\pi \times 2.5$ MHz, $Q \simeq 5 \times 10^6$, and $C_0 \simeq 4$ pF. Assuming the same Be^+ trap conditions as in Appendix B, we require $N \simeq l_i/L_Q \simeq 50\,000$ to make $l_N \simeq l_Q$. C_T is in parallel with the much larger quartz-resonator electrode capacitance C_0. Therefore $C_T \rightarrow C_0$ in Fig. 11. Adjusting the laser cooling to make $R_N = 1/\omega C_T$, we numerically evaluate the energy in the source mode $\langle i_s^2 \rangle L_s$ to be equivalent to a temperature $\langle i_s^2 \rangle L_s/k_B \simeq 35$ mK, where we have assumed that $T_s = 4.2$ K. Since crystals with much higher Q's (lower values of R_Q) might be obtained, perhaps much lower values of temperature might eventually be reached. For example, Ref. 64 reports a 1-MHz crystal with a Q of 4×10^9 at a temperature of 2 K. If this same Q could be obtained on our example crystal, then $R_s \rightarrow 0.08$ Ω, and $\langle i_s^2 \rangle L_s/k_B = 0.54$ mK $\simeq T_N$.

By use of suitable mechanical transducers and/or of intermediate transfer oscillators, such as quartz crystals, macroscopic oscillators of much larger mass, such as gravitational antennas, may possibly be cooled. Detection of energy changes in these macroscopic resonators can then be detected by the reaction back on the ions as described previously.

[1] W. H. Louisell, A. Yariv, and A. E. Siegman, Phys. Rev. **124**, 1646 (1961).

[2] H. Heffner, Proc. IRE **50**, 1604 (1962).

[3] H. A. Haus and J. A. Mullen, Phys. Rev. **128**, 2407 (1962).

[4] C. M. Caves, Phys. Rev. D **26**, 1817 (1982).

[5] J. Weber, Rev. Mod. Phys. **31**, 681 (1959).

[6] N. Bloembergen, Phys. Rev. Lett. **2**, 84 (1959).

[7] H. Dehmelt, Bull. Am. Phys. Soc. **20**, 60 (1975).

[8] C. Hilbert and J. Clarke, J. Low Temp. Phys. **61**, 263 (1985); M. R. Freeman, R. S. Germain, R. C. Richardson, M. L. Roukes, W. J. Gallagher, and M. B. Ketchen, Appl. Phys. Lett. **48**, 300 (1986).

[9] R. M. Weisskoff, G. P. Lafyatis, K. R. Boyce, E. A. Cornell, R. W. Flanagan, Jr., and D. E. Pritchard, J. Appl. Phys. **63**, 4599 (1988).

[10] M. F. Bocko, Rev. Sci. Instrum. **55**, 256 (1984).

[11] S. R. Jefferts and F. L. Walls, Rev. Sci. Instrum. **60**, 1194 (1989).

[12] H. G. Dehmelt, Adv. At. Mol. Phys. **3**, 53 (1967); **5**, 109 (1969).

[13] D. J. Wineland, Wayne M. Itano, and R. S. VanDyck, Jr., Adv. At. Mol. Phys. **19**, 135 (1983).

[14] F. Diedrich, J. C. Bergquist, Wayne M. Itano, and D. J. Wineland, Phys. Rev. Lett. **62**, 403 (1989).

[15] E. Amaldi and G. Pizzela, in *Relativity, Quanta and Cosmology*, edited by M. Pantaleo and R. De Finis (Johnson Reprint Corp., New York, 1979), Vol. 1, p. 9.

[16] V. B. Braginsky and A. B. Manukin, in *Measurements of Weak Forces in Physics Experiments*, edited by David H. Douglas (University of Chicago Press, Chicago, 1977).

[17] V. B. Braginsky, V. P. Mitrofanov, and V. I. Panov, *Systems with Small Dissipation*, translated by Erast Gliner (University of Chicago Press, Chicago, 1986).

[18] J. E. Moody and F. Wilczek, Phys. Rev. D **30**, 130 (1984).

[19] D. J. Larson, J. C. Bergquist, J. J. Bollinger, Wayne M. Itano, and D. J. Wineland, Phys. Rev. Lett. **57**, 70 (1986).

[20] J. J. Bollinger, D. J. Heinzen, Wayne M. Itano, S. L. Gilbert, and D. J. Wineland, Phys. Rev. Lett. **63**, 1031 (1989).

[21] F. Diedrich (private communication).

[22] D. J. Wineland, Wayne M. Itano, J. C. Bergquist, S. L. Gilbert, J. J. Bollinger, and F. Ascarrunz, in *Non-Neutral Plasma Physics*, Proceedings of the Symposium on Non-Neutral Plasma Physics held at the National Academy of Sciences, 1988, Conf. Proc. No. 175, edited by C. W. Roberson and C. F. Driscoll (AIP, New York, 1988), p. 93.

[23] L. S. Brown and G. Gabrielse, Rev. Mod. Phys. **58**, 233 (1986).

[24] D. J. Wineland, J. J. Bollinger, and Wayne M. Itano, Phys. Rev. Lett. **50**, 628 (1983).

[25] R. S. VanDyck, Jr., F. L. Moore, D. L. Farnham, and P. B. Schwinberg, in *Frequency Standards and Metrology, Proceedings of the Fourth Symposium*, Ancona, Italy, 1988, edited by A. DeMarchi (Springer-Verlag, Berlin, 1989), p. 349.

[26] E. A. Cornell, R. M. Weisskoff, K. R. Boyce, R. W. Flanagan, Jr., G. P. Lafyatis, and D. E. Pritchard, Phys. Rev. Lett. **63**, 1674 (1989).

[27] R. S. Van Dyck, Jr., P. B. Schwinberg, and H. G. Dehmelt, in *New Frontiers in High-Energy Physics*, edited by B. M. Kursunoglu, A. Perlmutter, and L. F. Scott (Plenum, New York, 1978), p. 159; R. S. Van Dyck, Jr., P. B. Schwinberg, and H. G. Dehmelt, Phys. Rev. Lett. **59**, 26 (1987).

[28] P. B. Schwinberg, R. S. VanDyck, Jr., and H. G. Dehmelt, Phys. Lett. **81A**, 119 (1981).

[29] G. Gabrielse, X. Fei, L. A. Orozco, R. L. Tjoelker, J. Haas, H. Kalinowsky, T. A. Trainor, and W. Kells, Phys. Rev. Lett. **63**, 1360 (1989).

[30] D. F. Walls, Nature **306**, 141 (1983), and references therein.

[31]I. Fujiwara and K. Miyoshi, Prog. Theor. Phys. **64**, 715 (1980); W. Schleich and J. A. Wheeler, J. Opt. Soc. Am. B **4**, 1715 (1987).

[32]J. C. Bergquist, F. Diedrich, Wayne M. Itano, and D. J. Wineland, in *Laser Spectroscopy IX,* edited by M. S. Feld, J. E. Thomas, and A. Mooradian (Academic, San Diego, 1989), p. 274.

[33]W. Shockley, J. Appl. Phys. **9**, 635 (1938).

[34]D. J. Wineland and H. G. Dehmelt, J. Appl. Phys. **46**, 919 (1975).

[35]M. A. Philip, F. Gelbard, and S. Arnold, J. Coll. Int. Sci. **91**, 507 (1983); G. Gabrielse, Phys. Rev. A **29**, 462 (1984); E. C. Beaty, Phys. Rev. A **33**, 3645 (1986).

[36]M. Lax, Phys. Rev. **145**, 110 (1966).

[37]D. J. Wineland, Wayne M. Itano, J. C. Bergquist, and R. G. Hulet, Phys. Rev. A **36**, 2220 (1987).

[38]W. Neuhauser, M. Hohenstatt, P. Toschek, and H. Dehmelt, Phys. Rev. Lett. **41**, 233 (1978).

[39]D. J. Wineland and Wayne M. Itano, Phys. Rev. A **20**, 1521 (1979).

[40]L. Allen and J. H. Eberly, *Optical Resonance and Two-Level Atoms* (Wiley, New York, 1975), Sec. 3.2.

[41]W. Nagourney, J. Sandberg, and H. Dehmelt, Phys. Rev. Lett. **56**, 2797 (1986).

[42]D. J. Wineland, J. C. Bergquist, Wayne M. Itano, and R. E. Drullinger, Opt. Lett. **5**, 245 (1980).

[43]J. C. Bergquist, Randall G. Hulet, Wayne M. Itano, and D. J. Wineland, Phys. Rev. Lett. **57**, 1699 (1986).

[44]Th. Sauter, W. Neuhauser, R. Blatt, and P. E. Toschek, Phys. Rev. Lett. **57**, 1696 (1986).

[45]Wayne M. Itano and D. J. Wineland, Phys. Rev. A **25**, 35 (1982).

[46]E. A. Cornell, R. M. Weisskoff, K. R. Boyce, and D. E. Pritchard, Phys. Rev. A **41**, 312 (1990).

[47]R. S. Van Dyck, Jr., F. L. Moore, D. L. Farnham, and P. B. Schwinberg, Rev. Sci. Instrum. **57**, 593 (1986).

[48]H. Dehmelt, Ann. Phys. (Paris) **10**, 777 (1985).

[49]L. S. Brown, G. Gabrielse, J. Tan, and K. C. D. Chan, Phys. Rev. A **37**, 4163 (1988); L. S. Brown, G. Gabrielse, K. Helmerson, and J. Tan, Phys. Rev. Lett. **55**, 44 (1985); L. S. Brown, in *Themes in Contemporary Physics II,* edited by S. Deser and R. J. Finkelstein (World Scientific, Singapore, 1989).

[50]J. Tan and G. Gabrielse, Appl. Phys. Lett. **55**, 2144 (1989).

[51]R. S. VanDyck, Jr., F. L. Moore, D. L. Farnham, and P. B. Schwinberg, Int. J. Mass Spectrom Ion Proc. **66**, 327 (1985).

[52]E. R. Cohen and B. N. Taylor, in *The 1986 Adjustment of the Fundamental Physical Constants,* Report of the CODATA Task Group on Fundamental Constants, CODATA Bulletin No. 63 (Pergamon, Elmsford, NY, 1986).

[53]H. G. Dehmelt and F. L. Walls, Phys. Rev. Lett. **21**, 127 (1968).

[54]V. B. Braginsky, Y. I. Vorontsov, and K. S. Thorne, Science **209**, 547 (1980).

[55]S. Stenholm, Rev. Mod. Phys. **58**, 699 (1986).

[56]D. J. Wineland and W. M. Itano, Phys. Today 40(6), 34 (1987).

[57]H. Dehmelt, G. Janik, and W. Nagourney, Bull. Am. Phys. Soc. **30**, 111 (1988).

[58]P. E. Toschek and W. Neuhauser, J. Opt. Soc. Am. B **6**, 2220 (1989).

[59]Markus Lindberg and Juha Javanainen, J. Opt. Soc. Am. B **3**, 1008 (1986).

[60]Murray Sargent, III, and Paul Horwitz, Phys. Rev. A **13**, 1962 (1976).

[61]Wayne M. Itano and D. J. Wineland, Phys. Rev. A **24**, 1364 (1981).

[62]Courtesy of R. Wallace and K. C. Dominic Chan, Accelerator Theory and Simulation Group, Los Alamos National Laboratory.

[63]P. Kartaschoff, *Frequency and Time* (Academic, London, 1978), p. 41.

[64]A. G. Smagin, Prib. Tekh. Eksp. **17** (6), 143 (1974).